

# PRODUCT OPERATOR FORMALISM FOR THE DESCRIPTION OF NMR PULSE EXPERIMENTS

O. W. SØRENSEN, G. W. EICH, M. H. LEVITT, G. BODENHAUSEN and R. R. ERNST  
Laboratorium für Physikalische Chemie, Eidgenössische Technische Hochschule, 8092 Zürich,  
Switzerland

(Received 29 March 1983)

## CONTENTS

1. Introduction	163
2. Approaches for the Analysis of Pulse Experiments	164
2.1. Classical vector models	164
2.2. Semiclassical vector models	164
2.3. Density operator approach	164
2.4. Product operator formalism	165
3. Nomenclature of Product Operators	166
4. Pictorial Representations of Product Operators	167
5. Evolution of Product Operators	169
5.1. Chemical shifts	171
5.2. Spin-spin couplings	172
5.3. Radio-frequency pulses	172
5.4. Pulses with arbitrary phase	173
5.5. Pulses with tilted rf fields	174
6. Composite Rotations	175
7. Magnetic Equivalence	178
8. Spins with $S > 1/2$	179
9. Multiple Quantum Coherence	181
10. Observables	183
11. Semiselective and Selective Pulses	184
12. Two-Dimensional Correlation Spectroscopy	185
13. Relayed Magnetization Transfer	186
14. Multiple Quantum Spectroscopy	187
15. Multiple Quantum Filters	188
16. Zero Quantum Interference in 2D Exchange Spectroscopy	189
17. Signal Intensities for Non-Equilibrium Systems	189
18. Conclusions	190
Acknowledgements	190
References	191

## 1. INTRODUCTION

In recent years, an astonishing variety of pulse techniques has been developed with the aim of enhancing the information content or the sensitivity of NMR spectra in both solution and solid phases.<sup>(1–39)</sup> For the design and analysis of new techniques two approaches have been pursued in the field of “spin engineering”. Many of the original concepts were based on simplified *classical or semiclassical vector models* which have inherently severe limitations for describing more sophisticated techniques; for example, those involving multiple quantum coherence. On the other hand, for a full analysis of arbitrarily complex pulse experiments applied to large spin systems, the heavy machinery of *density operator theory* has been put into action, often at the expense of physical intuition.

We present here an approach which follows a middle course. It is founded on density operator theory but retains the intuitive concepts of the classical or semiclassical vector models. The formalism systematically uses product operators to represent the state of the spin system.



In Section 2 we discuss the relation of product operators to vector models and density operator theory. In the following three sections, we develop the nomenclature of product operators, the relationship between operators and vector pictures, and the rules for the evolution under shifts, couplings and pulses. Combinations of evolution intervals and rf pulses are treated in Section 6 in terms of “composite rotations”. Magnetically equivalent nuclei are discussed in Section 7. The scalar coupling to nuclei with spin  $S > 1/2$  and the effects of quadrupolar couplings in anisotropic phase are the subject of Section 8. In Section 9, multiple-quantum coherence is discussed in terms of shift operators and of single-spin operators. Guidelines are indicated in Section 10 for deriving the observable magnetization, in particular the amplitudes and phases of multiplets. Selective pulses are briefly mentioned in Section 11. Finally, we treat in Sections 12–15 some examples involving coherence transfer such as two-dimensional correlation spectroscopy, relayed magnetization transfer, multiple quantum filters, 2D exchange spectroscopy, and systems with non-uniform spin temperature in the context of flip angle effects.

## 2. APPROACHES FOR THE ANALYSIS OF PULSE EXPERIMENTS

### 2.1. Classical Vector Models

In systems containing only isolated nuclei without spin–spin coupling (and without quadrupolar coupling), the magnetization can be described in terms of Bloch equations as a classical vector moving in three-dimensional space. This approach is satisfactory to describe many basic experiments of Fourier spectroscopy,<sup>(1)</sup> including spin-echoes,<sup>(2)</sup>  $T_1$  measurements,<sup>(3)</sup> “DANTE” sequences,<sup>(9,10)</sup> composite pulses,<sup>(27,28)</sup> measurement of slow chemical exchange<sup>(22,38)</sup> and spin imaging.<sup>(39)</sup>

### 2.2. Semiclassical Vector Models

In multi-level systems, it is possible to assign a vector to each individual transition. The effects of selective pulses and precession can still be understood on classical grounds. However, non-classical extensions are necessary to describe the transfer of coherence from one transition to another.<sup>(6)</sup> In this context, the substitution of non-selective pulses by pulse cascades has proved to be convenient.<sup>(40)</sup> Semiclassical vector models, though successful for many experiments, including heteronuclear 2D spectroscopy<sup>(14–16)</sup> and other polarization transfer experiments,<sup>(17–19)</sup> must be handled with care. In particular vector models do not adequately reflect the interdependence of z-components belonging to single transitions that share common energy levels.

### 2.3. Density Operator Approach

In contrast to semiclassical treatments, the quantum mechanical approach does not deal directly with observable magnetization, but rather with the state of the spin system, irrespective of the observable that will be finally detected.<sup>(41–43)</sup> The state of the system is expressed either by the wave function  $\psi(t)$  or by the density operator  $\sigma(t)$ .

If relaxation is disregarded, the time evolution of the density operator is described by the Liouville–von Neumann equation

$$\dot{\sigma}(t) = -i[\mathcal{H}(t), \sigma(t)]. \quad (1)$$

The Hamiltonian includes chemical shift terms, coupling terms and interactions with time-dependent external radio-frequency fields. It can be made time-independent within a finite time segment by selecting a suitable rotating frame. The time evolution can then be expressed by a sequence of unitary transformations of the type:

$$\sigma(t + \tau_1 + \tau_2) = \exp\{-i\mathcal{H}_2\tau_2\} \exp\{-i\mathcal{H}_1\tau_1\} \sigma(t) \exp\{+i\mathcal{H}_1\tau_1\} \exp\{+i\mathcal{H}_2\tau_2\} \quad (2)$$

with the propagators  $\exp\{-i\mathcal{H}_k\tau_k\}$ . This equation applies to any sequence of intervals  $\tau_k$  with constant external fields, or alternatively to  $\tau_k$  intervals where a time-independent average Hamiltonian  $\bar{\mathcal{H}}_k$  can be defined.



Having computed the time evolution of the density operator  $\sigma(t)$ , the observable magnetization components can be evaluated from the trace relations:

$$M_x(t) = \mathcal{N}\gamma\hbar \text{Tr} \{F_x\sigma(t)\}; \quad M_y(t) = \mathcal{N}\gamma\hbar \text{Tr} \{F_y\sigma(t)\} \quad (3)$$

with the number of nuclei per unit volume  $\mathcal{N}$  and the observable operators

$$F_x = \sum_k I_{kx}; \quad F_y = \sum_k I_{ky} \quad (4)$$

which are evaluated by summation over all spins  $k$  of one particular kind (for example protons, carbon-13, etc.). We shall discuss the implications of these trace relations in Section 10, with particular emphasis on the behaviour of individual multiplet components in coupled spin systems.

The evaluation of expectation values according to eqns. (3) takes place in the so-called ‘‘Schrödinger representation’’ where the state of the system represented by the density operator  $\sigma(t)$  is time-dependent, while the observable operators are time-independent. Sometimes, it is more convenient to transfer the time dependence to the observable operator, e.g.  $F_x$ , in the sense

$$\begin{aligned} M_x(t) &= \mathcal{N}\gamma\hbar \text{Tr} \{F_x(U(t)\sigma(0)U^{-1}(t))\} \\ &= \mathcal{N}\gamma\hbar \text{Tr} \{(U^{-1}(t)F_xU(t))\sigma(0)\} \\ &= \mathcal{N}\gamma\hbar \text{Tr} \{F_x(t)\sigma(0)\}. \end{aligned} \quad (5)$$

Attributing the time-dependence to the operators amounts to using the so-called ‘‘Heisenberg representation’’,<sup>(44)</sup> where in analogy to eqn. [2] the evolution is described by

$$F_x(t + \tau_1 + \tau_2) = \exp \{i\mathcal{H}_1\tau_1\} \exp \{i\mathcal{H}_2\tau_2\} F_x(t) \exp \{-i\mathcal{H}_2\tau_2\} \exp \{-i\mathcal{H}_1\tau_1\}. \quad (6)$$

Note the opposite order of the propagators. The Heisenberg representation, though it provides less intuitive insight, is of advantage when the evolution should be discussed for various initial conditions  $\sigma(0)$ . As long as relaxation is not considered both representations are only trivially different. However, for proper consideration of relaxation and exchange processes it is necessary to work in the Schrödinger representation. In the following, we use only the ‘‘natural’’ Schrödinger representation although the formalism can equally well be applied to the Heisenberg representation.

When eqn. (2) is expressed in terms of explicit matrices the unitary transformations amount to multiplications of matrices with dimension  $2^N \times 2^N$  for  $N$  spins with  $I = 1/2$ . In the eigenbasis of the unperturbed Hamiltonian, the elements of the density matrix have a simple physical meaning: a diagonal element  $\sigma_{ii}(t)$  represents the population  $P_i(t)$  of energy level  $i$ , while an off-diagonal element  $\sigma_{ij}$  represents coherence belonging to the transition  $(i,j)$ . Free precession can be readily described in the eigenbase, since the propagator  $\exp \{-i\mathcal{H}\tau\}$  is represented by a diagonal matrix, but the matrix elements of pulse operators cause complicated mixing of the matrix elements of  $\sigma(t)$ .<sup>(5,6)</sup> Explicit matrix representations tend to be cumbersome for systems with more than a few coupled spins.

## 2.4. Product Operator Formalism

For the evaluation of eqns. (2)–(6) the density operator  $\sigma$  may be expressed as a linear combination of base operators  $B_s$ :<sup>(41)</sup>

$$\sigma(t) = \sum_s b_s(t)B_s. \quad (7)$$

The complexity of practical calculations greatly depends on the choice of the set  $\{B_s\}$ . The use of irreducible tensor operators as base operators has been proposed elsewhere.<sup>(45,46)</sup> Single transition operators,<sup>(47,48)</sup> which are useful to describe selective excitation, can also be used as base operators, but in the case of non-selective excitation retain much of the complexity of explicit matrix calculations.

To provide at the same time physical insight and computational convenience, we propose to express the density operator systematically in terms of product operators:

$$B_s = 2^{(q-1)} \prod_{k=1}^N (I_{kv})^{a_k} \quad (8)$$



where  $N$  = total number of  $I = 1/2$  nuclei in the spin system,  $k$  = index of nucleus,  $v = x, y$  or  $z$ ,  $q$  = number of single-spin operators in the product,  $a_{sk} = 1$  for  $q$  nuclei and  $a_{sk} = 0$  for the  $N - q$  remaining nuclei.

Product operators for spin  $1/2$  nuclei are orthogonal with respect to formation of the trace, however they are not normalized, i.e.

$$\text{Tr} \{B_r B_s\} = \delta_{r,s} 2^{N-2}. \quad (9)$$

The complete base set  $\{B_s\}$  for a system with  $N$  spins  $1/2$  consists of  $4^N$  product operators  $B_s$ .

As an example, we list the complete set of 16 product operators  $B_s$  for a two-spin system:

$$\begin{aligned} q = 0 & \quad \frac{1}{2}E \quad (E = \text{unity operator}) \\ q = 1 & \quad I_{1x}, I_{1y}, I_{1z}, I_{2x}, I_{2y}, I_{2z} \\ q = 2 & \quad 2I_{1x}I_{2x}, 2I_{1x}I_{2y}, 2I_{1x}I_{2z}, \\ & \quad 2I_{1y}I_{2x}, 2I_{1y}I_{2y}, 2I_{1y}I_{2z}, \\ & \quad 2I_{1z}I_{2x}, 2I_{1z}I_{2y}, 2I_{1z}I_{2z}. \end{aligned}$$

Any arbitrary density operator can be expressed as a linear combination of such a set of base operators. At first sight, the bewildering array of terms seems discouraging. Yet this choice greatly simplifies calculations of pulse experiments applied to weakly-coupled systems, because the destiny of individual operator terms can be followed throughout the experiment and can be associated with a clear physical meaning.

The effects of free precession and of rf pulses are described by a sequence of transformations of the type:

$$\exp \{-i\phi B_r\} B_s \exp \{i\phi B_r\} = \sum_i b_{is}(r, \phi) B_i. \quad (10)$$

where  $\phi B_r$  takes the form  $(\Omega_k \tau) I_{kz}$  for chemical shift precession,  $(\pi J_{k\ell} \tau) 2I_{kz} I_{\ell z}$  for the evolution under weak scalar coupling between two spins with  $I = 1/2$ , and  $\beta I_{kv}$  for an rf pulse applied to nucleus  $k$  with rotation angle  $\beta$  and rotation axis  $v$ .

### 3. NOMENCLATURE OF PRODUCT OPERATORS

The nomenclature proposed in this section is chosen in view of the relevance of product operators for the observed spectrum. We assume a high resolution Hamiltonian where the individual spin multiplets are resolved.

In the context of an  $N$ -spin system, we distinguish one-spin, two-spin and generally  $q$ -spin product operators. *One-spin operators* are associated with entire spin multiplets.  $I_{kz}$  represents  $z$ -magnetization with equal polarization across all transitions of spin  $k$ . The transverse operators  $I_{kx}$  and  $I_{ky}$  are representative of the spin  $k$  multiplet with all multiplet components in-phase along the  $x$ - or  $y$ -axes of the rotating frame. This suggests the following nomenclature:

$I_{kz}$ : longitudinal magnetization of spin  $k$ ,

$I_{kx}$ : in-phase  $x$ -magnetization of spin  $k$ ,

$I_{ky}$ : in-phase  $y$ -magnetization of spin  $k$ .

The *two-spin product operators* can be classified as follows:

$2I_{kx}I_{\ell z}$ : antiphase  $x$ -magnetization of spin  $k$ , or more specifically,  $x$ -magnetization of spin  $k$  antiphase with respect to spin  $\ell$ ,

$2I_{ky}I_{\ell z}$ : antiphase  $y$ -magnetization of spin  $k$ , or more specifically  $y$ -magnetization of spin  $k$  antiphase with respect to spin  $\ell$ ,

$2I_{kx}I_{\ell x}$ ,  $2I_{ky}I_{\ell y}$ ,  $2I_{kx}I_{\ell y}$  and  $2I_{ky}I_{\ell x}$ : two-spin coherence of spins  $k$  and  $\ell$ ,

$2I_{kz}I_{\ell z}$ : longitudinal two-spin order of spins  $k$  and  $\ell$ .



Antiphase magnetization represents multiplets with individual components that have opposite phases. For example,  $2I_{kx}I_{\ell z}$  corresponds to a  $k$ -spin multiplet with magnetization components along the  $+x$  or  $-x$  axis of the rotating frame, depending on the polarization of spin  $\ell$ . An antiphase multiplet has zero integrated intensity. Two-spin coherence represents a superposition of zero and double quantum coherence, as will be discussed in Section 9. "Longitudinal spin order" refers to spin-correlated population of energy levels without net polarization and without observable magnetization.

In larger spin systems of  $I = 1/2$  nuclei, *three-spin product operators* may appear in the following forms:

- $4I_{kx}I_{\ell z}I_{mz}$ :  $x$ -magnetization of spin  $k$ , in antiphase with respect to the spins  $\ell$  and  $m$ ,
- $4I_{kx}I_{\ell x}I_{mz}$ : two-spin coherence of spins  $k$  and  $\ell$ , in antiphase with respect to spin  $m$ ,
- $4I_{kx}I_{\ell x}I_{mx}$ : three-spin coherence,
- $4I_{kz}I_{\ell z}I_{mz}$ : longitudinal three-spin order.

Antiphase two-spin coherence comprises zero quantum and double quantum coherence with multiplet components that have opposite phases depending on the polarization  $I_{mz}$  of the "passive" spin  $m$ . Three-spin coherence consists of a superposition of single quantum coherence (combination lines) and of triple quantum coherence (see Section 9).

We should note that the expression "magnetization" is used only for observable single quantum transitions. "Coherence", on the other hand, can refer either to transverse single quantum magnetization or to multiple quantum coherence.

#### 4. PICTORIAL REPRESENTATIONS OF PRODUCT OPERATORS

The product operators discussed above can readily be related to semiclassical vector models. In a system with two spins  $k$  and  $\ell$ , the in-phase magnetization  $I_{kx}$  may be represented as shown in Fig. 1 by parallel vectors along the positive  $x$ -axis in the rotating frame, or alternatively by parallel arrows in the energy level diagram. (We use wavy lines to distinguish coherence from a flow of population.)

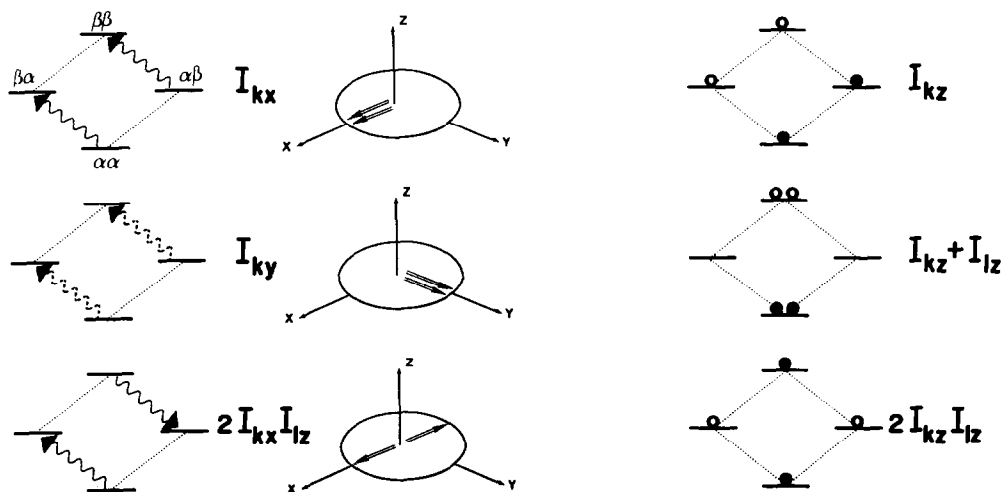


Fig. 1. Graphical representations of product operators representing single-quantum magnetization and longitudinal magnetization in a system of two coupled nuclei with  $I = 1/2$ . The oscillating  $x$  and  $y$  magnetization components are represented by wavy lines in the energy-level diagram (dashed lines for  $y$  components) or by the customary vectors in the  $xy$ -plane of the rotating frame. Populations are represented symbolically by open symbols for states that are depleted, filled symbols for states that are more populated than in the demagnetized saturated state.



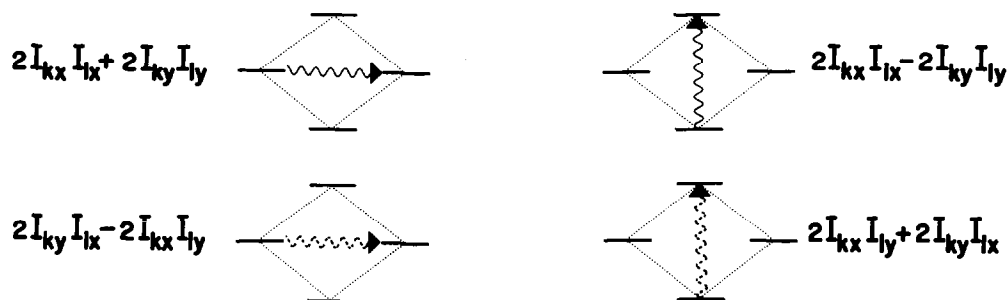


FIG. 2. Graphical representation of the linear combinations of product operators that represent pure zero- and double-quantum coherence in a two-spin system with  $I = 1/2$ . The wavy lines are solid or dashed depending on the phase of the coherence. Simple products never represent pure  $p$ -quantum coherence, for example,  $2I_{kx}I_{lx}$  amounts to a superposition of two diagrams.

Negative components are represented by reversing the sign of the arrows in either picture, while  $y$ -components can be indicated in the energy level diagram by dashed wavy arrows ( $I_{ky}$  in Fig. 1). Antiphase single quantum magnetization is represented by antiparallel vectors ( $2I_{kx}I_{lx}$  in Fig. 1).

Longitudinal magnetization and spin-spin order is indicated by filled and open symbols for positive and negative deviations from the equally populated, demagnetized state ( $I_{kz}$ ,  $I_{kz} + I_{lz}$ ,  $2I_{kz}I_{lz}$  in Fig. 1).

In principle, the population differences across individual transitions can also be represented by  $z$ -magnetization components in vector diagrams. Although this approach is valuable in discussing polarization transfer,<sup>(16-19)</sup> it must be used with great care as it does not reflect the fact that several transitions may share common energy levels.

Figure 2 shows how pure zero- and double quantum operators (see Section 9) may be represented graphically. Again, dashed wavy arrows are used to indicate  $y$  components. Although some authors

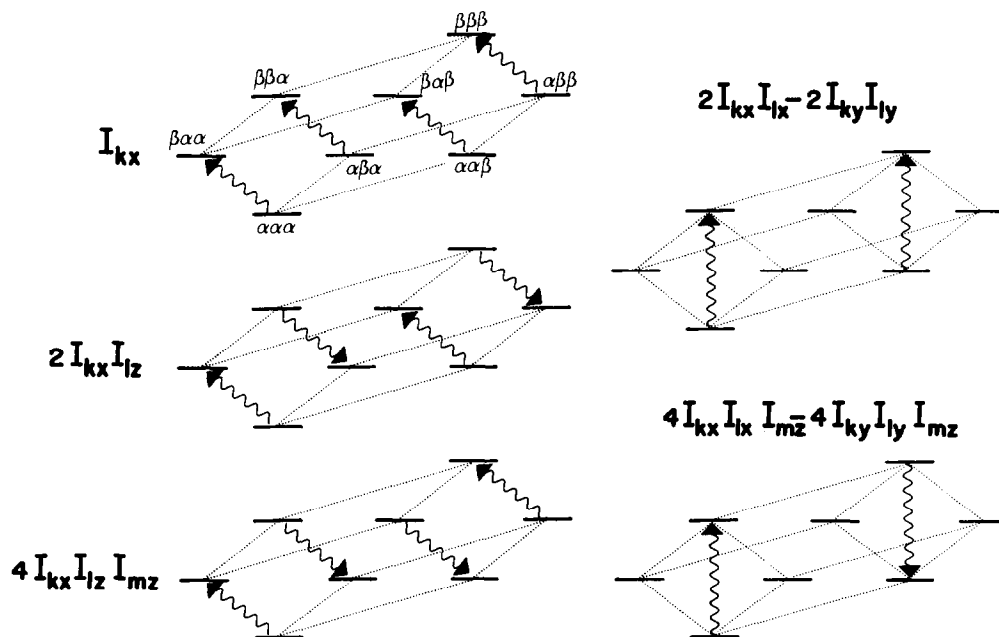


FIG. 3. Graphical representations of some product operators corresponding to single and double quantum coherence in a system of three coupled spins with  $I = 1/2$ . The arrows indicate parallel and antiparallel coherence components. Note that each term represents an entire multiplet rather than an individual transition.



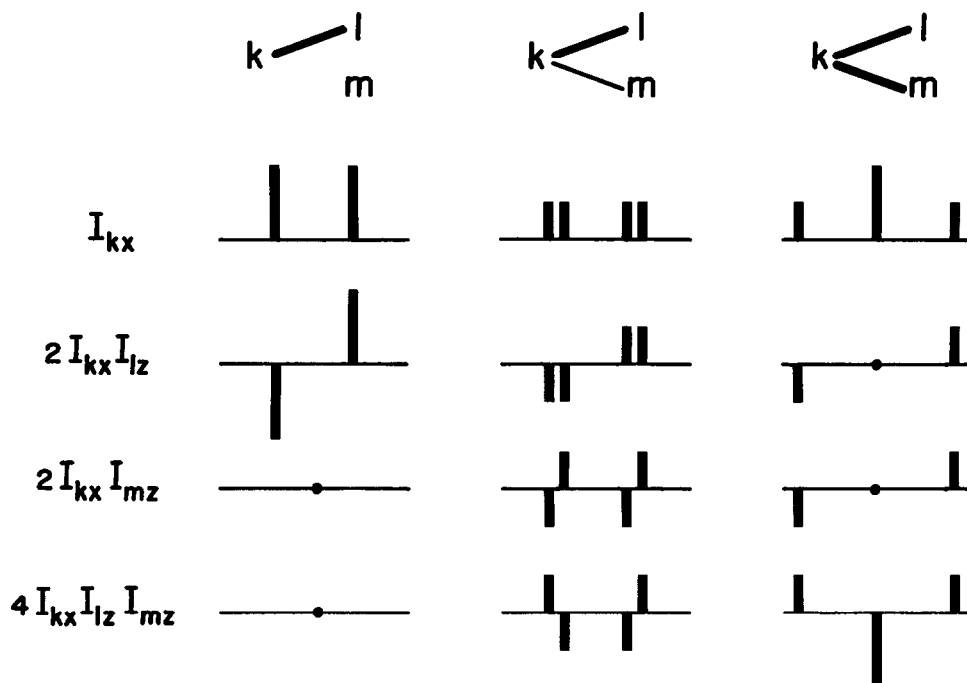


FIG. 4. Schematic spectra obtained after Fourier transformation of the free induction decays induced by some typical product operators involving single quantum coherence of nucleus  $k$  in a system with three spins with  $I = 1/2$ . In linear networks ( $J_{km} = 0$ ), magnetization of spin  $k$  antiphase with respect to spin  $m$  is not observable (bottom left). In systems with degenerate couplings (right column), the central transition vanishes if two components with opposite phase are superimposed. Linear combinations of product operators yield operators that correspond to single transitions. Thus the sum of all four stick spectra in the central column yields a single line on the right (see Section 11).

have represented multiple quantum coherence by vectors,<sup>(32,49)</sup> we prefer to restrict the use of vector models to observable magnetization.

Figure 3 gives pictorial representations of a few typical product operators that may occur in three-spin systems: in-phase magnetization  $I_{kx}$ , antiphase magnetization with respect to one or two couplings, ( $2I_{kx}I_{lz}$ ,  $4I_{kx}I_{lz}I_{mz}$ ), pure in-phase double quantum coherence involving two of the three spins, ( $2I_{kx}I_{lx} - 2I_{ky}I_{ly}$ ), and pure double quantum coherence in antiphase with respect to the third (passive) spin,  $2(2I_{kx}I_{lx} - 2I_{ky}I_{ly})I_{mz}$ .

These examples demonstrate that the product operators are easy to visualise and are closely related to semiclassical pictorial representations. There is also a direct relation between the appearance of the spectrum and the presence of observable product operators. Four examples are shown in Fig. 4 for three-spin systems with different coupling patterns. A more detailed discussion of the relationship between multiplet patterns and product operators is given in Section 10.

## 5. EVOLUTION OF PRODUCT OPERATORS

We restrict the discussion of the time evolution of product operators to weakly coupled spin systems, since strong coupling complicates the situation without providing more insight into the mechanism of pulse experiments. In most cases, the treatment of strongly coupled systems requires a numerical computer analysis (see for example Ref. 50). For weakly coupled systems, on the other hand, analytical calculations are straightforward. Throughout, we shall use a shorthand notation to express



evolution caused by the Hamiltonian. Equation (2) will be expressed in the form

$$\sigma(t) \xrightarrow{\mathcal{H}_1 \tau_1} \sigma(t + \tau_1) \xrightarrow{\mathcal{H}_2 \tau_2} \sigma(t + \tau_1 + \tau_2) \quad (11)$$

where the algebraic signs and the chronological sequence of the transformations correspond to the arguments of the time-ordered exponential operators on the *right hand side* of eqn. (2). (The imaginary unit  $i$  is dropped in this notation.)

First consider the evolution of the density operator under the unperturbed weak coupling Hamiltonian

$$\begin{aligned} \mathcal{H} &= \sum_k \Omega_k I_{kz} + \sum_{k < \ell} \sum_{\ell} 2\pi J_{k\ell} I_{kz} I_{\ell z} \\ &= \sum_k \Omega_k (I_{kz}) + \sum_{k < \ell} \sum_{\ell} \pi J_{k\ell} (2I_{kz} I_{\ell z}). \end{aligned} \quad (12)$$

Note that the Hamiltonian is written in terms of the product operators  $B_s$  defined in eqn. (8) by a trivial rearrangement of the factor 2. The shift frequency of nucleus  $k$  in the rotating frame is defined by  $\Omega_k = \omega_{0k} - \omega_{rf}$ , with the Larmor frequency  $\omega_{0k} = -\gamma_k(1 - \sigma_k)B_0$  and the rf frequency  $\omega_{rf}$ . In hetero-nuclear systems several different rf frequencies and rotating frames may be used.

We consistently define positive rotations (frequencies and angles) in the right-handed sense (clockwise). A positive rotation about the  $z$ -axis leads from  $x \rightarrow y \rightarrow -x \rightarrow -y$ . For positive gyromagnetic ratio, Larmor frequencies  $\omega_{0k}$  are negative if  $B_0$  is oriented along the positive  $z$ -axis. Magnetic field and rotation frequency vectors are antiparallel both in the laboratory as well as in the rotating frame as shown in Fig. 5.

Since all terms in eqn. (12) commute, the evolution caused by the individual terms can be computed separately in arbitrary order:

$$\begin{aligned} \sigma(t + \tau) &= \prod_k \exp(-i\Omega_k \tau I_{kz}) \prod_{k < \ell} \exp(-i\pi J_{k\ell} \tau 2I_{kz} I_{\ell z}) \sigma(t) \\ &\quad \times \prod_{k < \ell} \exp(i\pi J_{k\ell} \tau 2I_{kz} I_{\ell z}) \prod_k \exp(i\Omega_k \tau I_{kz}) \end{aligned} \quad (13a)$$

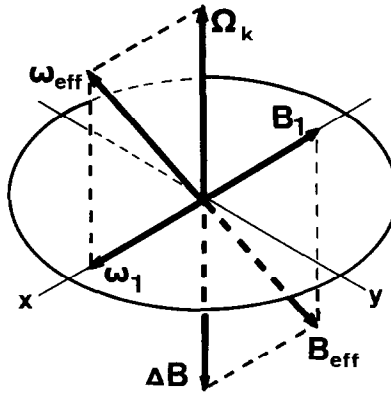


FIG. 5. Magnetic field vector  $\Delta B_k = (1 - \sigma_k)B_0 + \omega_{rf}/\gamma$  and precession frequency vector  $\Omega_k = \omega_{0k} - \omega_{rf}$  in the rotating frame for a case where the carrier frequency  $|\omega_{rf}|$  is placed above the resonance frequency  $|\omega_{0k}|$  (for  $\gamma > 0$ ). The chemical shift precession frequency  $\Omega_k$  is in this case represented by a vector parallel to the positive  $z$ -axis. The resulting effective magnetic field vector  $B_{eff}$  and effective precession frequency vector  $\omega_{eff}$  are indicated for an rf field  $B_1$  applied along the negative  $x$ -axis. The corresponding rotation vector  $\omega_1 = -\gamma B_1$  points then along the positive  $x$ -axis and induces a positive rotation, i.e.  $z \rightarrow -y \rightarrow -z \rightarrow y$ .



or symbolically:

$$\sigma(t) \xrightarrow{\Omega_1 \tau I_{1z}} \xrightarrow{\Omega_2 \tau I_{2z}} \dots \xrightarrow{\pi J_{12} \tau 2I_{1z} I_{2z}} \xrightarrow{\pi J_{13} \tau 2I_{1z} I_{3z}} \dots \sigma(t + \tau). \quad (13b)$$

One may speak of a "cascade of chemical shift terms" and a "cascade of coupling terms" in analogy to pulse cascades.<sup>(40)</sup> The transformations under the action of shifts, couplings and pulses will now be discussed separately.

### 5.1. Chemical Shifts

The effect of a shift frequency  $\Omega_k$  is described by

$$I_{kx} \xrightarrow{\Omega_k \tau I_{kz}} I_{kx} \cos \Omega_k \tau + I_{ky} \sin \Omega_k \tau \quad (14)$$

$$I_{ky} \xrightarrow{\Omega_k \tau I_{kz}} I_{ky} \cos \Omega_k \tau - I_{kx} \sin \Omega_k \tau. \quad (15)$$

These transformations are shown graphically in Fig. 6.

For a product operator representing two-spin coherence, for example, we obtain the following chemical shift evolution:

$$2I_{kx}I_{\ell x} \xrightarrow{\Omega_k \tau I_{kz}} \xrightarrow{\Omega_\ell \tau I_{\ell z}} 2(I_{kx} \cos \Omega_k \tau + I_{ky} \sin \Omega_k \tau)(I_{\ell x} \cos \Omega_\ell \tau + I_{\ell y} \sin \Omega_\ell \tau). \quad (16)$$

Clearly,  $\Omega_k \tau I_{kz}$  only affects  $I_{kx}$ , and  $\Omega_\ell \tau I_{\ell z}$  only affects  $I_{\ell x}$  in this cascade.

Chemical shift evolution always conserves the number  $q$  of operators  $I_{kv}$  in each term  $B_s$ . An

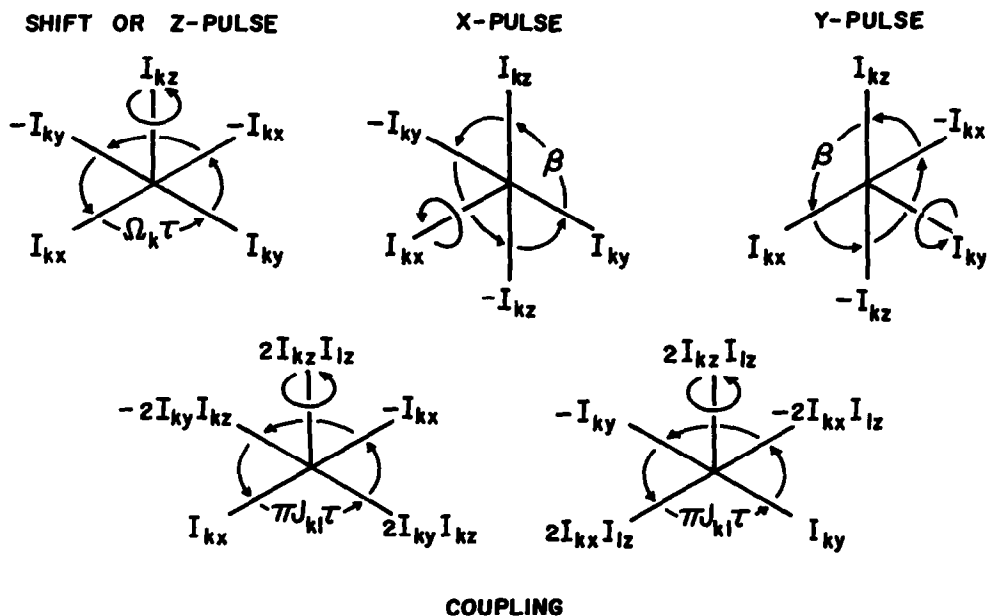


FIG. 6. The effect of chemical shifts, on-resonance rf pulses, and positive scalar couplings on product operators. These figures are based on commutator relationships that are applicable to arbitrary spins  $I_k \geq 1/2$  with a coupling partner with spin  $I_\ell = 1/2$ . They represent three-dimensional operator subspaces within which rotations take place in complete analogy to rotations in three-dimensional physical space. The sense of rotation is indicated for positive rotation angles.



operator with  $q_i$  transverse components ( $I_{kx}, I_{ky}$ ) transforms into a linear combination of at most  $2^q$  terms, while the longitudinal components  $I_{kz}$  remain invariant.

### 5.2. Spin-Spin Couplings

For a coupling between two nuclei  $k$  and  $\ell$  within an arbitrary network of coupled spins  $I = 1/2$  we find the rules:

$$I_{kx} \xrightarrow{\pi J_{k\ell} \tau 2I_{kz} I_{\ell z}} I_{kx} \cos(\pi J_{k\ell} \tau) + 2I_{ky} I_{\ell z} \sin(\pi J_{k\ell} \tau) \quad (17)$$

$$I_{ky} \xrightarrow{\pi J_{k\ell} \tau 2I_{kz} I_{\ell z}} I_{ky} \cos(\pi J_{k\ell} \tau) - 2I_{kx} I_{\ell z} \sin(\pi J_{k\ell} \tau). \quad (18)$$

This corresponds to the conversion of in-phase magnetization into orthogonal antiphase magnetization. If we start out with antiphase magnetization, the evolution under the scalar coupling generates in-phase magnetization:

$$2I_{kx} I_{\ell z} \xrightarrow{\pi J_{k\ell} \tau 2I_{kz} I_{\ell z}} 2I_{kx} I_{\ell z} \cos(\pi J_{k\ell} \tau) + I_{ky} \sin(\pi J_{k\ell} \tau) \quad (19)$$

$$2I_{ky} I_{\ell z} \xrightarrow{\pi J_{k\ell} \tau 2I_{kz} I_{\ell z}} 2I_{ky} I_{\ell z} \cos(\pi J_{k\ell} \tau) - I_{kx} \sin(\pi J_{k\ell} \tau). \quad (20)$$

These equations are restricted to nuclei with  $I_\ell = 1/2$ , but include cases with  $I_k > 1/2$ . They can be derived by the procedure outlined by Slichter,<sup>(42)</sup> using the cyclic commutation relationships

$$[2I_{kz} I_{\ell z}, I_{ky}] = -i2I_{kx} I_{\ell z}. \quad (21)$$

The transformations in eqns. (17)–(20) are depicted schematically in Fig. 6.

### 5.3. Radio-Frequency Pulses

First, we restrict the discussion to strong non-selective rf pulses with  $|\omega_1| = |\gamma B_1| \gg |\Omega_k| \gg |\pi J_{k\ell}|$ . The effect of pulses with phase  $\nu = x$  or  $y$  and flip angle  $\beta$  is represented by the transformation:

$$\sigma(t_+) = \exp\left(-i\beta \sum_k I_{k\nu}\right) \sigma(t_-) \exp\left(+i\beta \sum_k I_{k\nu}\right) \quad (22)$$

where the summation is carried out over all spins affected by the pulse (possibly restricted to either  $I$  or  $S$  species in heteronuclear systems). In shorthand notation one may write in arbitrary order:

$$\sigma(t_-) \xrightarrow{\beta I_{k\nu}} \xrightarrow{\beta I_{\ell\nu}} \xrightarrow{\beta I_{m\nu}} \dots \sigma(t_+). \quad (23)$$

The effect of an rf pulse can be considered separately for each single-spin operator  $I_{k\nu}$  in the product operators.

For a rotation about the  $x$ -axis one obtains:

$$I_{kz} \xrightarrow{\beta I_{kx}} I_{kz} \cos \beta - I_{ky} \sin \beta \quad (24)$$

$$I_{ky} \xrightarrow{\beta I_{kx}} I_{ky} \cos \beta + I_{kz} \sin \beta, \quad (25)$$

and for a rotation about the  $y$ -axis:

$$I_{kz} \xrightarrow{\beta I_{ky}} I_{kz} \cos \beta + I_{kx} \sin \beta \quad (26)$$

$$I_{kx} \xrightarrow{\beta I_{ky}} I_{kx} \cos \beta - I_{kz} \sin \beta. \quad (27)$$



One should keep in mind that a positive rotation angle  $\beta$  indicates rotation in the right-handed (clockwise) sense, as illustrated in Fig. 6. This logical choice of the sense of rotation<sup>(51,52)</sup> is opposite to a convention widely used in NMR.<sup>(42,53)</sup> By “x-pulse”, we understand a rotation about a vector  $\omega_1 = -\gamma B_1$  aligned along the positive x-axis. Thus for nuclei with positive gyromagnetic ratio, the rf field is, in this case, actually aligned along the negative x-axis. In practice, it is of course the rotation vector  $\omega_1$  which determines the outcome of the experiment. Thus, we consider it natural to indicate the direction of the rotation vector rather than the direction of the rf field. However, in the vast majority of NMR experiments, the actual sense of physical rotation of magnetization vectors cannot be determined and hence the choice of convention is rather academic.

With rf phase shifts or pulse sandwiches<sup>(27,28)</sup> it is also possible to create the equivalent of z-pulses<sup>(54)</sup> and achieve the following transformations:

$$I_{kx} \xrightarrow{\beta I_{kz}} I_{kx} \cos \beta + I_{ky} \sin \beta \quad (28)$$

$$I_{ky} \xrightarrow{\beta I_{kz}} I_{ky} \cos \beta - I_{kx} \sin \beta. \quad (29)$$

These transformations are analogous to the effect of chemical shifts shown in Fig. 6.

As an example of a y-pulse, consider the effect on a two-spin operator representing antiphase magnetization:

$$2I_{kx}I_{\ell z} \xrightarrow{\frac{\pi}{2}(I_{ky} + I_{\ell y})} -2I_{kz}I_{\ell x}. \quad (30)$$

This expresses the transfer of antiphase magnetization of nucleus  $k$  into antiphase magnetization of nucleus  $\ell$ , a process which is the key to many coherence transfer experiments.

On the other hand, if an x-pulse is applied to the same antiphase magnetization:

$$2I_{kx}I_{\ell z} \xrightarrow{\frac{\pi}{2}(I_{kx} + I_{\ell x})} -2I_{kx}I_{\ell y} \quad (31)$$

one obtains a transfer into two-spin coherence, a phenomenon that is exploited in zero and double quantum spectroscopy.

#### 5.4. Pulses with Arbitrary Phase

Pulses with arbitrary phase  $\varphi$  (defined as the displacement from the x-axis towards the y-axis) can be represented by the transformation

$$\sigma(t_+) = \exp \left\{ -i\beta \sum_k [I_{kx} \cos \varphi + I_{ky} \sin \varphi] \right\} \sigma(t_-) \times \exp \left\{ +i\beta \sum_k [I_{kx} \cos \varphi + I_{ky} \sin \varphi] \right\} \quad (32)$$

$$\begin{aligned} &= \exp \left( -i\varphi \sum_k I_{kz} \right) \exp \left( -i\beta \sum_k I_{kx} \right) \exp \left( +i\varphi \sum_k I_{kz} \right) \sigma(t_-) \\ &\quad \times \exp \left( -i\varphi \sum_k I_{kz} \right) \exp \left( +i\beta \sum_k I_{kx} \right) \exp \left( +i\varphi \sum_k I_{kz} \right). \end{aligned} \quad (33)$$

Thus the effect of a pulse with phase  $\varphi$  and flip angle  $\beta$  on an arbitrary initial condition may be calculated in three separate steps (expressing the operators on the right-hand side of eqn. (33) in shorthand notation):

$$\sigma(t_-) \xrightarrow{-\varphi \sum_k I_{kz}} \xrightarrow{\beta \sum_k I_{kx}} \xrightarrow{\varphi \sum_k I_{kz}} \sigma(t_+). \quad (34)$$



The first operation corresponds to a z-pulse with rotation angle  $-\varphi$ , the second to an x-pulse with flip angle  $\beta$ , and the final step is a z-pulse with rotation angle  $\varphi$ . Equations (24)–(27) can thus be generalized for arbitrary phase  $\varphi$ :

$$I_{kz} \xrightarrow{\beta[I_{kx} \cos \varphi + I_{ky} \sin \varphi]} I_{kz} \cos \beta + I_{kx} \sin \beta \sin \varphi - I_{ky} \sin \beta \cos \varphi \quad (35)$$

$$I_{kx} \xrightarrow{\beta[I_{kx} \cos \varphi + I_{ky} \sin \varphi]} -I_{kz} \sin \beta \sin \varphi + I_{kx} (\cos \beta \sin^2 \varphi + \cos^2 \varphi) + I_{ky} \sin^2 \beta / 2 \sin 2\varphi \quad (36)$$

$$I_{ky} \xrightarrow{\beta[I_{kx} \cos \varphi + I_{ky} \sin \varphi]} I_{kz} \sin \beta \cos \varphi + I_{kx} \sin^2 \beta / 2 \sin 2\varphi + I_{ky} (\cos \beta \cos^2 \varphi + \sin^2 \varphi). \quad (37)$$

In practice, one can achieve such transformations either by applying a single pulse shifted in phase through an angle  $\varphi$ , or alternatively by using pulse sandwiches.<sup>(54)</sup>

### 5.5. Pulses with Tilted RF Fields

The effects of tilted rf fields can be calculated in an analogous manner. For a pulse with flip angle  $\beta$ , arbitrary phase  $\varphi$  and tilt angle  $\theta$  away from the z-axis, the transformation may be written in five steps:

$$\sigma(t_-) \xrightarrow{-\varphi \sum_k I_{kz}} \xrightarrow{\left(\frac{\pi}{2} - \theta\right) \sum_k I_{ky}} \xrightarrow{+\beta \sum_k I_{kx}} \xrightarrow{-\left(\frac{\pi}{2} - \theta\right) \sum_k I_{ky}} \xrightarrow{+\varphi \sum_k I_{kz}} \sigma(t_+). \quad (38)$$

Note that on-resonance pulses correspond to  $\theta = \pi/2$ . In this manner we obtain general relations:

$$\begin{aligned} I_{kz} \xrightarrow{\beta, \varphi, \theta} & I_{kz} [\cos \beta \sin^2 \theta + \cos^2 \theta] \\ & + I_{kx} [\sin \beta \sin \varphi \sin \theta + \sin^2 \beta / 2 \cos \varphi \sin 2\theta] \\ & + I_{ky} [-\sin \beta \cos \varphi \sin \theta + \sin^2 \beta / 2 \sin \varphi \sin 2\theta] \end{aligned} \quad (39)$$

$$\begin{aligned} I_{kx} \xrightarrow{\beta, \varphi, \theta} & I_{kz} [\sin^2 \beta / 2 \sin 2\theta \cos \varphi - \sin \beta \sin \varphi \sin \theta] \\ & + I_{kx} [\cos \beta (\sin^2 \varphi + \cos^2 \varphi \cos^2 \theta) + \cos^2 \varphi \sin^2 \theta] \\ & + I_{ky} [\sin^2 \beta / 2 \sin 2\theta \sin^2 \varphi + \sin \beta \cos \varphi \sin \theta] \end{aligned} \quad (40)$$

$$\begin{aligned} I_{ky} \xrightarrow{\beta, \varphi, \theta} & I_{kz} [\sin^2 \beta / 2 \sin 2\theta \sin \varphi + \sin \beta \cos \varphi \sin \theta] \\ & + I_{kx} [\sin^2 \beta / 2 \sin 2\theta \sin^2 \varphi - \sin \beta \cos \varphi \sin \theta] \\ & + I_{ky} [\cos \beta (\cos^2 \varphi + \sin^2 \varphi \cos^2 \theta) + \sin^2 \varphi \sin^2 \theta]. \end{aligned} \quad (41)$$

These equations are useful to predict the effect of non-ideal pulses. Consider for example the effect of a tilted refocussing pulse on a state of pure double quantum coherence (see Section 9). The effective flip angle, defined by  $\beta = -\tau\gamma\sqrt{B_1^2 + \Delta B_0^2}$  and assumed identical for both nuclei, is set to  $\beta = \pi$ . If the rf phase is set to  $\varphi = 0$  for clarity, the following transformation is obtained:

$$(I_{kx} I_{\ell y} + I_{ky} I_{\ell x}) \xrightarrow{\beta = \pi, \varphi = 0, \theta} (I_{kx} I_{\ell y} + I_{ky} I_{\ell x}) \cos 2\theta - (I_{kz} I_{\ell y} + I_{ky} I_{\ell z}) \sin 2\theta. \quad (42)$$



The second term implies that even with an ideal flip angle  $\beta = \pi$ , the double quantum coherence is partly converted into antiphase single quantum magnetization. Artifacts resulting from such undesirable coherence transfer phenomena may be cancelled by appropriate phase-cycling techniques.<sup>(26)</sup>

## 6. COMPOSITE ROTATIONS

It is often useful to treat certain groups of pulses and precession intervals as single units which have a simple overall effect. Typically, such units appear as symmetrical sandwiches. This approach has been used extensively to describe selective multiple-quantum excitation<sup>(55)</sup> and time-reversal experiments.<sup>(56)</sup> We shall restrict the discussion to a few cases relevant for weakly-coupled systems.

(1) A simple example is a "composite z-pulse",<sup>(54)</sup> mentioned in the previous section (eqns. (28) and (29)), which consists of the sequence  $(\pi/2)_- \beta_y (\pi/2)_+$  and can be represented in shorthand:

$$\sigma(t_-) \xrightarrow{-\frac{\pi}{2} \sum_k I_{kx}} \xrightarrow{\beta \sum_k I_{ky}} \xrightarrow{+\frac{\pi}{2} \sum_k I_{kx}} \sigma(t_+). \quad (43)$$

Since

$$\exp\left(-i\frac{\pi}{2} I_{kx}\right) \exp(+i\beta I_{ky}) \exp\left(+i\frac{\pi}{2} I_{kx}\right) = \exp(i\beta I_{kz}), \quad (44)$$

the overall effect of the three pulses may be written in condensed form

$$\sigma(t_-) \xrightarrow{\beta \sum_k I_{kz}} \sigma(t_+), \quad (45)$$

which amounts to a rotation about the z-axis through an angle  $\beta$ . Such composite z-pulses can be used to simulate a continuously-variable phase shift of the rf carrier.<sup>(54)</sup>

(2) Some experiments require that the multiplet components evolve under the exclusive influence of the spin-spin coupling term. For this purpose an evolution period of length  $2\tau$  is interrupted by a  $\pi$  pulse to refocus chemical shifts. The effect of such a  $\tau - (\pi)_x - \tau$  sequence on the density operator is a composite rotation which may be written in shorthand:

$$\sigma(t_-) \xrightarrow{\sum \pi J_{kl} \tau 2I_{kz} I_{lz}} \xrightarrow{\sum \Omega_k \tau I_{kz}} \xrightarrow{\pi \sum I_{kx}} \xrightarrow{\sum \Omega_k \tau I_{kz}} \xrightarrow{\sum \pi J_{kl} \tau 2I_{kz} I_{lz}} \sigma(t + 2\tau_+). \quad (46)$$

Because of the relationship

$$e^{i\Omega_k \tau I_{kz}} e^{i\pi I_{kx}} = e^{i\pi I_{kx}} e^{-i\Omega_k \tau I_{kz}} \quad (47)$$

one may swap the second and third terms in eqn. (46) while changing the sign of the shift term. Thus the effect of shifts is cancelled, and, since the coupling and inversion terms commute, one obtains the equivalent transformation

$$\sigma(t_-) \xrightarrow{\pi \sum_k I_{kx}} \xrightarrow{\sum \pi J_{kl} 2\tau 2I_{kz} I_{lz}} \sigma(t + 2\tau_+). \quad (48)$$

A similar simplification is obtained for a  $\pi$ -pulse with arbitrary phase  $\varphi$ . Equation (48) shows that the  $\pi$ -pulse may be thought of as if it were applied at the beginning of the  $2\tau$ -interval. If the initial state is described by  $I_{kx}$  terms, a  $(\pi)_x$  pulse will have no effect, while a  $(\pi)_y$  pulse reverses the sign.

(3) In other experiments, the refocussing sequence is bracketed by two  $\pi/2$  pulses. Thus the effect of the sequence  $(\pi/2)_x - \tau - (\pi)_x - \tau - (\pi/2)_x$  may be written, using eqn. (48):

$$\sigma(t_-) \xrightarrow{\frac{3\pi}{2} \sum_k I_{kx}} \xrightarrow{\sum \pi J_{kl} 2\tau 2I_{kz} I_{lz}} \xrightarrow{\frac{\pi}{2} \sum_k I_{kx}} \sigma(t + 2\tau_+). \quad (49)$$



This expression can be simplified to

$$\sigma(t_-) \xrightarrow{\sum \pi J_{kl} 2\tau 2I_{ky}I_{ly}} \sigma(t+2\tau_+). \quad (50)$$

Thus the overall effect of the  $(\pi/2)_x - \tau - (\pi)_x - \tau - (\pi/2)_x$  sequence is described by a bilinear rotation about the  $y$ -axis which causes the transformations:

$$I_{kz} \xrightarrow{\sum \pi J_{kl} 2\tau 2I_{ky}I_{ly}} I_{kz} \cos(\pi J_{kl} 2\tau) + 2I_{kx}I_{ly} \sin(\pi J_{kl} 2\tau) \quad (51)$$

$$I_{kx} \xrightarrow{\sum \pi J_{kl} 2\tau 2I_{ky}I_{ly}} I_{kx} \cos(\pi J_{kl} 2\tau) - 2I_{kz}I_{ly} \sin(\pi J_{kl} 2\tau). \quad (52)$$

These transformations are shown schematically in Fig. 7. Density operator components proportional to  $I_{ky}$  remain invariant under this rotation.

Equation (51) describes the creation of two-spin coherence from thermal equilibrium, whereas in eqn. (52) antiphase magnetization of spin  $\ell$  is generated from in-phase  $I_{kx}$  magnetization.

The effect of the analogous phase-shifted pulse sequence  $(\pi/2)_y - \tau - (\pi)_y - \tau - (\pi/2)_y$  is:

$$\sigma(t_-) \xrightarrow{\sum \pi J_{kl} 2\tau 2I_{kx}I_{lx}} \sigma(t+2\tau_+). \quad (53)$$

The transformations associated with such evolution operators, which are shown in Fig. 7, can be readily derived from the cyclic commutation relationships

$$[I_{k\lambda}, 2I_{k\mu}I_{\ell\xi}] = i2I_{k\nu}I_{\ell\xi} \quad (54)$$

with  $\lambda, \mu, \nu = x, y, z$  and cyclic permutations, and  $\xi = x, y$  or  $z$ .

## COMPOSITE ROTATIONS

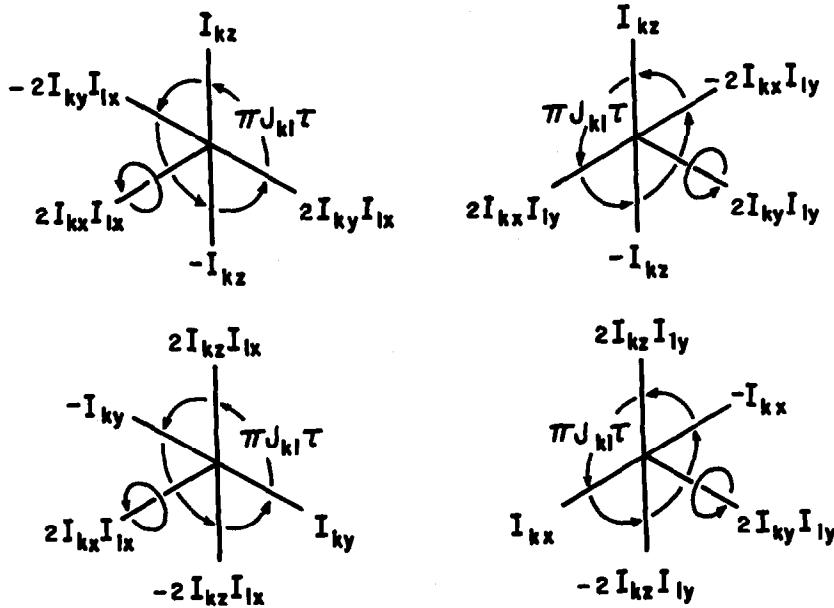


FIG. 7. Evolution of typical operator terms under the effect of product operators obtained in composite rotation sequences corresponding to effective Hamiltonians  $2I_{kx}I_{lx}$  and  $2I_{ky}I_{ly}$  respectively. The sense of rotation is indicated for  $J_{kl} > 0$ .



(4) Some pulse sequences use precession intervals without refocussing pulses, so that the chemical shift evolution must be considered as well. Thus a  $(\pi/2)_x - \tau - (\pi/2)_{-x}$  sequence can be described by

$$\sigma(t_-) \xrightarrow{\sum \pi J_{kl} \tau 2I_{ky} I_{ly}} \xrightarrow{\sum \Omega_k \tau I_{ky}} \sigma(t + \tau_+). \quad (55)$$

(5) Other sequences do not possess inherent "sandwich symmetry" but may be modified by inserting "dummy" pulses that have no effect on the density operator to introduce the symmetry required for simplifying the expressions. Thus the sequence commonly employed for odd-quantum excitation, which may be written  $(\pi/2)_x - \tau - (\pi)_y - \tau - (\pi/2)_y$ , can be expanded by inserting two dummy pulses:  $(\pi/2)_x (\pi/2)_{-y} (\pi/2)_y - \tau - (\pi)_y - \tau - (\pi/2)_y$ . In this modified form, the sandwich-sequence is easily recognized and the effect of the entire sequence is

$$\sigma(0_-) \xrightarrow{\frac{\pi}{2} \sum I_{kx}} \xrightarrow{-\frac{\pi}{2} \sum I_{ky}} \xrightarrow{\sum \pi J_{kl} 2\tau 2I_{kx} I_{lx}} \sigma(2\tau_+). \quad (56)$$

If the first pulse is applied to a system in thermal equilibrium, it generates pure  $-I_{ky}$  magnetization which is not affected by the second term in the cascade. Note that the pulse sequence  $(\pi/2)_x (\pi/2)_{-y}$  is equivalent to the sequence  $(\pi/2)_x (\pi/2)_x$ .

(6) In heteronuclear systems,  $\pi$ -pulses are often applied to both species  $I$  and  $S$  to prevent refocussing of the heteronuclear coupling terms. Thus the sequence  $(\pi/2)_x^I - \tau - (\pi)_x^{I,S} - \tau - (\pi/2)_x^I$  may be described:

$$\sigma(t_-) \xrightarrow{\pi \sum S_{mx}} \xrightarrow{\sum \pi J_{kl} 2\tau 2I_{ky} I_{ly}} \xrightarrow{\sum \pi J_{km} 2\tau 2I_{ky} S_{mz}} \sigma(t + 2\tau_+). \quad (57)$$

Note the appearance of terms  $I_{kv} S_{m\mu}$  with  $v \neq \mu$ , which occur because the  $\pi/2$  pulses act only on the  $I$  spins. The evolution of the density operator under such rotations is apparent from the commutation properties, eqn. (54), and may be represented diagrammatically in analogy to Fig. 6, by changing the axes of rotation to those labeled with  $2I_{ky} I_{lz}$  and  $2I_{kx} I_{lz}$ .

(7) Many experiments employ extensive phase cycling to select desirable coherence transfer pathways. For example, in the sequence commonly used for even-quantum excitation  $(\pi/2)_\phi - \tau - (\pi)_\phi - \tau - (\pi/2)_\phi$  it is possible to cancel undesired coherences by cycling the phase  $\phi$  (see Section 14). The effect of such phase-shifted excitation sandwiches may be written concisely as

$$\sigma(0_-) \xrightarrow{-\sum \phi I_{kz}} \xrightarrow{\sum \pi J_{kl} 2\tau 2I_{ky} I_{ly}} \xrightarrow{+\phi \sum I_{kz}} \sigma(2\tau_+). \quad (58)$$

If the initial density operator contains only populations and zero-quantum coherence, the first transformation has no effect. Thus the phase-shift boils down to a  $z$ -pulse applied after the actual excitation sequence. This form of analysis obviates the need to perform separate calculations for each member of a set of phase-shifted excitation sequences.

(8) Some experiments employ flip angles  $\beta \neq \pi/2$  to separate contributions from different spin systems, for example in the DEPT sequence,<sup>(57,58)</sup> which is used for subspectral editing in carbon-13 spectroscopy. To clarify the inner workings of such experiments, it is often useful to expand a single pulse into a sandwich. Thus

$$\sigma(t_-) \xrightarrow{\beta \sum I_{kx}} \sigma(t_+) \quad (59)$$

is equivalent to

$$\sigma(t_-) \xrightarrow{-\frac{\pi}{2} \sum I_{ky}} \xrightarrow{\beta \sum I_{kz}} \xrightarrow{+\frac{\pi}{2} \sum I_{ky}} \sigma(t_+) \quad (60)$$

where it becomes apparent that the pulse  $(\beta)_x$  has a similar effect as two  $(\pi/2)_y$  rotations bracketing a  $(\beta)_z$  rotation (which is equivalent to a phase shift).



(9) In practice, rf pulses often deviate substantially from their nominal flip angles because of rf inhomogeneity, and offset effects cause undesirable complications. Composite pulses have been designed to achieve proper population inversion under non-ideal conditions.<sup>(27,28,59-61)</sup> Pulse sequences of the form  $(\beta)_{\theta,x}(\beta')_{\theta,y}(\beta)_{\theta,x}$  have proven to be very useful. The flip angle  $\beta$  has the nominal value  $\pi/2$ , whilst  $\beta'$  takes nominal values ranging from  $\pi$  to  $4\pi/3$  depending on the application.<sup>(59,60)</sup> To a good approximation the composite pulses accomplish the transformation

$$I_{kz} \xrightarrow{(\beta)_{\theta,x}(\beta')_{\theta,y}(\beta)_{\theta,x}} -I_{kz}, \quad (61)$$

which implies that, when applied to arbitrary initial conditions, the composite pulse can be replaced formally by the sequence of operations:

$$\sigma(t_-) \xrightarrow{\sum_k \varphi_k I_{kz}} \xrightarrow{\pi \sum_k I_{kx}} \xrightarrow{-\sum_k \varphi_k I_{kz}} \sigma(t_+). \quad (62)$$

This substitution differs from those given above in that it is approximate, with an accuracy dependent on the success of the composite pulse in compensating non-idealities.

The expression eqn. (62) contains effective phase shifts  $\varphi_k$  which may be dependent on offset  $\Omega_k$  and must in general be calculated by numerical methods. Complications arising from these undesirable rotations are best avoided in spin echo experiments by always employing an even number of refocussing pulse sandwiches, in which case the unwanted effective phase shifts cancel out.<sup>(61)</sup>

## 7. MAGNETIC EQUIVALENCE

Many calculations in high-resolution NMR can be simplified if symmetry-adapted wave functions are introduced to analyse systems with magnetic equivalence. In weakly-coupled systems, however, symmetrization often provides little advantage. It turns out that the analysis of pulse experiments is more straightforward if symmetrized wave functions are avoided. Thus an  $A_2X$  system, for example, is treated as an  $AA'X$  system with  $J_{AX} = J_{A'X}$  and  $J_{AA'} = 0$ . This approach has proven valuable in discussing multiple quantum NMR<sup>(62)</sup> and polarization transfer experiments.<sup>(58)</sup>

It is well known that in systems with magnetically equivalent nuclei  $k$  and  $\ell$ , the coupling  $2\pi J_{k\ell} \mathbf{I}_k \cdot \mathbf{I}_\ell$  commutes with all propagators and observable operators, and may therefore be ignored. Symmetrization may be of advantage if strong coupling occurs, if selective irradiation is applied (tickling, etc.) and if relaxation mechanisms are considered. When symmetrization is employed, expressions for group spins with  $I \geq 1$  must be used such as treated in the next section.

In some experiments, otherwise non-equivalent spins are made virtually equivalent for a finite time interval. This situation arises when magnetization initially prepared in a non-equilibrium state is subjected to a strong rf field of finite duration and is finally observed in the absence of irradiation, such as in the course of Hartmann-Hahn cross-polarization experiments in liquids,<sup>(63)</sup> or when decoupling is applied for a limited time in the course of an experiment.<sup>(64)</sup> In these cases it is necessary to retain the full coupling Hamiltonian  $2\pi J_{k\ell} \mathbf{I}_k \cdot \mathbf{I}_\ell$  to express the evolution of product operators under the spin-spin couplings. The relevant transformations can be derived from the cyclic commutation relation

$$[\mathbf{I}_k \mathbf{I}_\ell, I_{kx} - I_{\ell x}] = i(2I_{ky}I_{\ell z} - 2I_{kz}I_{\ell y}) \quad (63)$$

and from similar relations obtained by cyclic permutations of the indices  $x$ ,  $y$  and  $z$ .

Thus one obtains, for an irradiation interval of duration  $\tau$ :

$$(I_{kx} - I_{\ell x}) \xrightarrow{2\pi J_{k\ell} \tau \mathbf{I}_k \cdot \mathbf{I}_\ell} (I_{kx} - I_{\ell x}) \cos(2\pi J_{k\ell} \tau) + (2I_{ky}I_{\ell z} - 2I_{kz}I_{\ell y}) \sin(2\pi J_{k\ell} \tau) \quad (64)$$

and analogous transformations for cyclic permutations of  $x$ ,  $y$  and  $z$ . Here, the difference of the in-phase magnetization of two nuclei is transferred into two antiphase magnetization terms. Non-equilibrium populations involving terms such as  $I_{kz} - I_{\ell z}$ , are converted into zero-quantum coherence



( $2I_{kx}I_{\ell y} - 2I_{ky}I_{\ell x}$ ) (see Section 9). This type of transformation is essential in polarization transfer experiments in the rotating frame.<sup>(63)</sup>

### 8. SPINS WITH $S > 1/2$

The evolution of the doublet of a spin  $S_\ell > 1/2$  under the scalar coupling to a nucleus with  $I_k = 1/2$  is correctly described by eqns. (17)–(20). The  $I_k$ -spin multiplet however, which consists of  $(2S_\ell + 1)$  lines of equal amplitude, evolves in a manner that depends on the quantum number  $S_\ell$  of the coupling partner.

For  $S_\ell = 1$ , we decompose the  $I_k$  triplet into a central line and in-phase and antiphase magnetization of the outer lines:

$$\begin{aligned}(0, x, 0) &= I_{kx}(E_\ell - S_{\ell z}^2) \\ (0, y, 0) &= I_{ky}(E_\ell - S_{\ell z}^2) \\ (x, 0, x) &= I_{kx}S_{\ell z}^2 \\ (-x, 0, x) &= I_{kx}S_{\ell z} \\ (y, 0, y) &= I_{ky}S_{\ell z}^2 \\ (-y, 0, y) &= I_{ky}S_{\ell z}.\end{aligned}\tag{65a}$$

The central components are invariant to  $J_{k\ell}$ -coupling, and the outer lines evolve in analogy to doublets involving  $S_\ell = 1/2$  nuclei, but with twice the usual coupling constant:

$$(x, 0, x) \xrightarrow{2\pi J_{k\ell}\tau I_{kz}S_{\ell z}} (x, 0, x) \cos 2\pi J_{k\ell}\tau + (-y, 0, y) \sin 2\pi J_{k\ell}\tau.\tag{65b}$$

These transformations are summed up in Fig. 8.

If an arbitrary spin  $I_k \geq 1/2$  is coupled to a spin  $S_\ell = 3/2$  (which may be a group spin if  $AX_3$  groups are treated in terms of symmetrized eigenfunctions), the  $I$ -spin quartet can be decomposed into in-phase and antiphase magnetization with the inner and outer transitions of the quartet:

$$\begin{aligned}(0, x, x, 0) &= \frac{1}{2}I_{kx}\left[\frac{9}{4}E_\ell - S_{\ell z}^2\right] \\ (0, -x, x, 0) &= -I_{kx}S_{\ell z}\left[\frac{9}{4}E_\ell - S_{\ell z}^2\right] \\ (x, 0, 0, x) &= -\frac{1}{2}I_{kx}\left[\frac{1}{4}E_\ell - S_{\ell z}^2\right] \\ (-x, 0, 0, x) &= \frac{1}{3}I_{kx}S_{\ell z}\left[\frac{1}{4}E_\ell - S_{\ell z}^2\right]\end{aligned}\tag{66a}$$

and corresponding  $y$ -components.

The evolution under the scalar coupling can be described by rotations in two-dimensional subspaces analogous to those depicted in Fig. 8:

$$(0, x, x, 0) \xrightarrow{2\pi J_{k\ell}\tau I_{kz}S_{\ell z}} (0, x, x, 0) \cos \pi J_{k\ell}\tau + (0, -y, y, 0) \sin \pi J_{k\ell}\tau\tag{66b}$$

$$(x, 0, 0, x) \xrightarrow{2\pi J_{k\ell}\tau I_{kz}S_{\ell z}} (x, 0, 0, x) \cos 3\pi J_{k\ell}\tau + (-y, 0, 0, y) \sin 3\pi J_{k\ell}\tau.\tag{66c}$$

Apart from the three-fold effective  $J$ -coupling constant in the last expression, these transformations are analogous to those of doublets involving  $S_\ell = 1/2$  nuclei. The effects of chemical shifts and rf pulses on  $S_\ell > 1/2$  nuclei are correctly described by eqns. (14), (15) and (22)–(41).



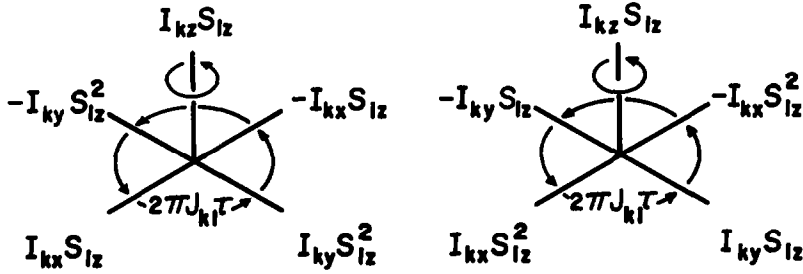
SCALAR COUPLING TO  $S = 1$ 

FIG. 8. Evolution of the outer magnetization components of a triplet of spin  $I_k$  coupled by  $J_{kl} > 0$  to a quadrupolar spin  $S_l = 1$ .

In the following, we demonstrate that the evolution under the quadrupolar Hamiltonian in solids or in liquid crystals can be treated in an analogous manner. We restrict the discussion to  $S = 1$  with an axially symmetric quadrupolar tensor ( $\eta = 0$ ) with the Hamiltonian:<sup>(42)</sup>

$$\mathcal{H}_Q = \frac{e^2 q Q}{4} (3S_z^2 - S^2) = \omega_Q (S_z^2 - \frac{1}{3}S^2) \quad (67a)$$

where  $\omega_Q$  corresponds to one-half of the quadrupolar splitting. Since the Hamiltonian  $\mathcal{H}_Q$  commutes with the weak coupling Hamiltonian of eqn. (12), quadrupolar evolution contributes another step in the "cascade" which describes free evolution in eqn. (13):

$$\sigma(t) \xrightarrow{\omega_Q \tau S_z^2} \sigma(t + \tau). \quad (67b)$$

Using the procedure outlined by Slichter<sup>(42)</sup> and the cyclic commutation relationships

$$[S_z^2, S_x] = +i\{S_y S_z + S_z S_y\} \quad (68)$$

one obtains the transformations shown in Fig. 9:

$$S_x \xrightarrow{\omega_Q \tau S_z^2} S_x \cos \omega_Q \tau + \{S_y S_z + S_z S_y\} \sin \omega_Q \tau \quad (69a)$$

$$S_y \xrightarrow{\omega_Q \tau S_z^2} S_y \cos \omega_Q \tau - \{S_x S_z + S_z S_x\} \sin \omega_Q \tau. \quad (69b)$$

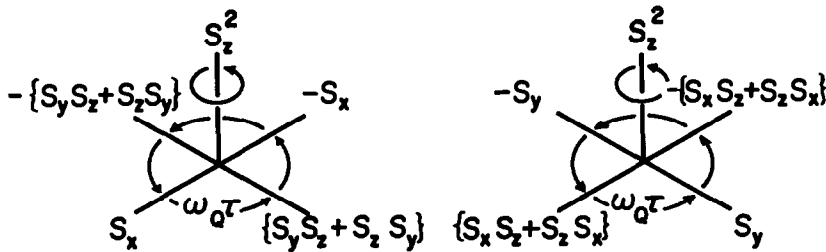
QUADRUPOLEAR COUPLING  $S = 1$ 

FIG. 9. Effect of the quadrupolar precession on the single-quantum magnetization components of an isolated spin  $S = 1$ .



In contrast to the product operators used in previous sections, products of the type  $S_x S_z$  which involve operators of the *same* spin are non-Hermitian and do not represent convenient basis operators  $B_s$  to expand the density operator. The expressions in curly brackets (anticommutators), however, are Hermitian. The terms  $\{S_x S_z + S_z S_x\}$  and  $\{S_y S_z + S_z S_y\}$  represent antiphase single-quantum magnetization of the quadrupolar doublet along the  $x$ - and  $y$ -axes, respectively.

The reader may easily verify that the sequence  $(\pi/2)_x - \tau - (\pi)_x - \tau - (\pi/2)_x$  generates a state of pure double-quantum coherence  $\{S_x S_y + S_y S_x\}$ , provided  $\tau = \pi/4\omega_Q$ .<sup>(65)</sup> The  $\pi$ -pulse eliminates the effect of chemical shift without modifying the precession under the quadrupolar coupling.

On the other hand, the sequence  $(\pi/2)_x - \tau - (\pi)_x - \tau - (\pi/2)_y - \tau' - (\pi)_x - \tau'$  leads to a state

$$\begin{aligned} \sigma(2\tau, 2\tau') = & S_y [\cos \omega_Q 2\tau \cos \omega_Q 2\tau' + \sin \omega_Q 2\tau \sin \omega_Q 2\tau'] \\ & + \{S_x S_z + S_z S_x\} [\sin \omega_Q 2\tau \cos \omega_Q 2\tau' - \cos \omega_Q 2\tau \sin \omega_Q 2\tau'] \end{aligned} \quad (70)$$

which contains only in-phase and antiphase single-quantum magnetization. For  $\tau' = \tau$ , at the quadrupolar echo, the full  $S_y$  magnetization is refocussed irrespective of the magnitude of the quadrupolar coupling. The same quadrupolar echo sequence may be expanded with dummy pulses in order to obtain composite rotation sandwiches:

$$[(\pi/2)_x - \tau - (\pi)_x - \tau - (\pi/2)_x] (\pi/2)_x [(\pi/2)_{-x} - \tau' - (\pi)_{-x} - \tau' - (\pi/2)_{-x}] (\pi/2)_x.$$

The two sandwiches represent pure quadrupolar evolution with the Hamiltonian  $\omega_Q S_y^2$ , and one immediately finds for each of the two sandwiches

$$S_z \xrightarrow{\omega_Q 2\tau S_y^2} S_z \cos \omega_Q 2\tau + (S_x S_y + S_y S_x) \sin \omega_Q 2\tau. \quad (71)$$

The evolution of the system in the course of the complete sequence is

$$\sigma(t) \xrightarrow{\omega_Q 2\tau S_y^2} \xrightarrow{\frac{\pi}{2} S_z} \xrightarrow{\omega_Q 2\tau' S_y^2} \xrightarrow{\frac{\pi}{2} S_x} \sigma(t + 2\tau + 2\tau'). \quad (72)$$

The phase shift operator  $(\pi/2)S_x$  does not affect the first but inverts the second term in eqn. (71), leading effectively to a time reversal and, after the full sequence, to the complete restoration of the initial magnetization at  $\tau' = \tau$ .

## 9. MULTIPLE QUANTUM COHERENCE

Product operators with  $q_t$  transverse single spin operators  $I_{kv}$  ( $v = x, y$ ) always consist of a superposition of multiple quantum coherences of orders  $p = q_t - 2n$  ( $n = 0, 1, 2, \dots$ ). This can be readily demonstrated by using raising and lowering operators:

$$I_{kx} = \frac{1}{2} (I_k^+ + I_k^-) \quad (73)$$

$$I_{ky} = \frac{1}{2i} (I_k^+ - I_k^-). \quad (74)$$

Thus two-spin product operators may be written:

$$2I_{kx}I_{lx} = \frac{1}{2} (I_k^+ I_l^+ + I_k^+ I_l^- + I_k^- I_l^+ + I_k^- I_l^-) \quad (75)$$

$$2I_{ky}I_{ly} = -\frac{1}{2} (I_k^+ I_l^+ - I_k^+ I_l^- - I_k^- I_l^+ + I_k^- I_l^-) \quad (76)$$

$$2I_{kx}I_{ly} = \frac{1}{2i} (I_k^+ I_l^+ - I_k^+ I_l^- + I_k^- I_l^+ - I_k^- I_l^-) \quad (77)$$



$$2I_{ky}I_{\ell x} = \frac{1}{2i}(I_k^+ I_\ell^+ + I_k^+ I_\ell^- - I_k^- I_\ell^+ - I_k^- I_\ell^-). \quad (78)$$

Clearly, all four product operators contain both double and zero quantum terms (concerted and opposite spin-flips respectively).

The linear combinations

$$\frac{1}{2}(2I_{kx}I_{\ell x} - 2I_{ky}I_{\ell y}) = \frac{1}{2}(I_k^+ I_\ell^+ + I_k^- I_\ell^-) = \{2QT\}_x \quad (79)$$

and

$$\frac{1}{2}(2I_{kx}I_{\ell y} + 2I_{ky}I_{\ell x}) = \frac{1}{2i}(I_k^+ I_\ell^+ - I_k^- I_\ell^-) = \{2QT\}_y \quad (80)$$

represent *pure double quantum coherence* and span a vector space in which double quantum coherence precesses under the influence of the sum of the chemical shifts:

$$\{2QT\}_x \xrightarrow{(\Omega_k I_{kz} + \Omega_\ell I_{\ell z})\tau} \{2QT\}_x \cos(\Omega_k + \Omega_\ell)\tau + \{2QT\}_y \sin(\Omega_k + \Omega_\ell)\tau. \quad (81)$$

Similarly, *pure zero quantum coherence* is given by

$$\frac{1}{2}(2I_{kx}I_{\ell x} + 2I_{ky}I_{\ell y}) = \frac{1}{2}(I_k^+ I_\ell^- + I_k^- I_\ell^+) = \{ZQT\}_x \quad (82)$$

$$\frac{1}{2}(2I_{ky}I_{\ell x} - 2I_{kx}I_{\ell y}) = \frac{1}{2i}(I_k^+ I_\ell^- - I_k^- I_\ell^+) = \{ZQT\}_y. \quad (83)$$

The precession is determined by the difference of the chemical shifts:

$$\{ZQT\}_x \xrightarrow{(\Omega_k I_{kz} + \Omega_\ell I_{\ell z})\tau} \{ZQT\}_x \cos(\Omega_k - \Omega_\ell)\tau + \{ZQT\}_y \sin(\Omega_k - \Omega_\ell)\tau. \quad (84)$$

*Pure triple quantum coherence* is easily described in terms of shift operators, which can be converted into Cartesian spin operators if necessary

$$\{3QT\}_x = \frac{1}{2}(I_k^+ I_\ell^+ I_m^+ + I_k^- I_\ell^- I_m^-) = \frac{1}{4}(4I_{kx}I_{\ell x}I_{mx} - 4I_{kx}I_{\ell y}I_{my} - 4I_{ky}I_{\ell x}I_{my} - 4I_{ky}I_{\ell y}I_{mx}) \quad (85)$$

$$\{3QT\}_y = \frac{1}{2i}(I_k^+ I_\ell^+ I_m^+ - I_k^- I_\ell^- I_m^-) = \frac{1}{4i}(4I_{ky}I_{\ell x}I_{mx} + 4I_{kx}I_{\ell y}I_{mx} + 4I_{kx}I_{\ell x}I_{my} - 4I_{ky}I_{\ell y}I_{my}). \quad (86)$$

The chemical shift evolution is:

$$\{3QT\}_x \xrightarrow{(\Omega_k I_{kz} + \Omega_\ell I_{\ell z} + \Omega_m I_{mz})\tau} \{3QT\}_x \cos(\Omega_k + \Omega_\ell + \Omega_m)\tau + \{3QT\}_y \sin(\Omega_k + \Omega_\ell + \Omega_m)\tau. \quad (87)$$

Arbitrary combination lines can be readily constructed in terms of shift operators. Thus a 4-spin-2-quantum coherence involving spins  $k$ ,  $\ell$ ,  $m$  and  $n$  with the fourth spin undergoing an opposite spin flip ( $\Delta m_n = -1$ ) is expressed by

$$\{4\text{-spin-}2QT\}_x = \frac{1}{2}(I_k^+ I_\ell^+ I_m^+ I_n^- + I_k^- I_\ell^- I_m^- I_n^+) \quad (88)$$

$$\{4\text{-spin-}2QT\}_y = \frac{1}{2i}(I_k^+ I_\ell^+ I_m^+ I_n^- - I_k^- I_\ell^- I_m^- I_n^+). \quad (89)$$



The precession under chemical shifts obeys the general rule

$$\{q\text{-spin-}pQT\}_x \xrightarrow{\sum \Omega_k I_{kz} \tau} \{q\text{-spin-}pQT\}_x \cos \Omega_{\text{eff}} \tau + \{q\text{-spin-}pQT\}_y \sin \Omega_{\text{eff}} \tau, \quad (90)$$

where

$$p = \Delta M = \sum_k \Delta m_k, \quad q = \sum_k |\Delta m_k|, \quad \Omega_{\text{eff}} = \sum_k \Delta m_k \Omega_k,$$

and  $\Delta m_k = \pm 1$  depending on the change in quantum number of spin  $k$ .<sup>(66)</sup>

The evolution of multiple quantum coherence is not affected by couplings between nuclei actively involved in the transition. For example, two-spin coherence is invariant to the transformation

$$2I_{kx}I_{\ell x} \xrightarrow{\pi J_{k\ell} \tau 2I_{kz}I_{\ell z}} 2I_{kx}I_{\ell x}. \quad (91)$$

This is consistent with the commutation expression

$$[2I_{k\lambda}I_{\ell\mu}, 2I_{k\mu}I_{\ell\xi}] = 0 \quad (92)$$

for  $\lambda = \mu$  and  $\nu = \xi$  or  $\lambda \neq \mu$  and  $\nu \neq \xi$ . On the other hand, multiple quantum coherence evolves under couplings to “passive” spins, leading to multiplets in the multiple quantum spectrum.

For  $q$ -spin- $p$ -quantum combination lines, the effective coupling constant with a passive nucleus  $m$  is defined in analogy to the effective chemical shift<sup>(66)</sup>

$$J_{\text{eff}} = \sum_k \Delta m_k J_{km}. \quad (93)$$

The evolution under the effective coupling is described by the transformation

$$\{q\text{-spin-}pQT\}_x \xrightarrow{\sum_k \pi J_{km} \tau 2I_{kz}I_{mz}} \{q\text{-spin-}pQT\}_x \cos \pi J_{\text{eff}} \tau + 2I_{mz} \{q\text{-spin-}pQT\}_y \sin \pi J_{\text{eff}} \tau. \quad (94)$$

The implications of rf phase-shifts or  $z$ -pulses are conveniently expressed in terms of shift operators:

$$e^{-i\varphi I_{kz}} I_k^+ e^{+i\varphi I_{kz}} = \exp(-i\varphi) I_k^+ \quad (95)$$

$$e^{-i\varphi I_{kz}} I_k^- e^{+i\varphi I_{kz}} = \exp(+i\varphi) I_k^-. \quad (96)$$

A  $p$ -quantum coherence term experiences a  $p$ -fold phase-shift:

$$\{q\text{-spin-}pQT\}_x \xrightarrow{\sum I_{kz}} \{q\text{-spin-}pQT\}_x \cos p\varphi + \{q\text{-spin-}pQT\}_y \sin p\varphi \quad (97)$$

Raising and lowering operators generally yield simpler expressions for higher-quantum coherences.

## 10. OBSERVABLES

As stated in eqn. (3) the observable transverse magnetization components are derived from the density operator  $\sigma(t)$  by forming the traces  $M_x(t) = \mathcal{N} \gamma \hbar \text{Tr} \{F_x \sigma(t)\}$  and  $M_y(t) = \mathcal{N} \gamma \hbar \text{Tr} \{F_y \sigma(t)\}$ . In fact, if we focus attention on systems with  $I = 1/2$  spins, exclusively one-spin operators of the type  $I_{kx}$  and  $I_{ky}$  give rise to observable magnetization. Products like  $2I_{kx}I_{\ell z}$ , representing antiphase magnetization, are not observable in a strict sense. In the course of the detection period, however, such antiphase product operators may evolve into observable in-phase magnetization:

$$2I_{kx}I_{\ell z} \xrightarrow{\pi J_{k\ell} \tau 2I_{kz}I_{\ell z}} [2I_{kx}I_{\ell z} \cos(\pi J_{k\ell} \tau) + I_{ky} \sin(\pi J_{k\ell} \tau)]. \quad (98)$$

After Fourier transformation, the observable term  $I_{ky} \sin(\pi J_{k\ell} \tau)$  leads to an *antiphase* doublet



centered at the chemical shift  $\Omega_k$ . Such a doublet is observable only when the two lines are resolved, since the two antiphase components cancel if the line width exceeds the magnitude of the coupling. All product operators which in the course of the detection period evolve into observable magnetization are henceforth referred to as "observables". In particular, all product operators containing a single transverse component  $I_{kx}$  or  $I_{ky}$  and an arbitrary number of longitudinal components, such as  $2I_{kx}I_{\ell z}$ ,  $4I_{kx}I_{\ell z}I_{mz}$ , ..., are observable, provided all couplings  $J_{k\ell}$ ,  $J_{km}$ , ... are resolved. However, if one of the couplings is insufficiently resolved, observation will be strongly inhibited.

The relative amplitudes and phases of the spectral lines can be derived immediately from the form of the product operators. Consider a system of three weakly coupled spins,  $k$ ,  $\ell$  and  $m$  with  $I = 1/2$ . Figure 4 illustrates the one-dimensional spectra of spin  $k$  obtained after Fourier transformation of a free induction signal induced by a number of typical product operators. For  $J_{k\ell} = J_{km}$ , the multiplet of nucleus  $k$  collapses to a triplet. Product operators are therefore easily visualized in terms of the spectra to which they give rise.

In systems with strong coupling, additional product operators corresponding to combination lines, like  $I_{kx}(I_{\ell x}I_{mx} + I_{\ell y}I_{my})$  also become observable. (See the expressions for zero quantum transitions, eqns. (82) and (83).) By contrast, multiple quantum coherence can never lead to observable magnetization unless further pulses are applied.

For heteronuclear  $IS$  systems with  $S > 1/2$  nuclei, the situation is slightly more complicated. For  $S = 1$ , the product operators  $I_{kx}$ ,  $I_{kx}S_{\ell z}$  and  $I_{kx}S_{\ell z}^2$  represent triplets with amplitudes  $(1, 1, 1)$ ,  $(-1, 0, 1)$  and  $(1, 0, 1)$  respectively. In addition, products containing even powers of transverse  $S_{\ell x}$  and  $S_{\ell y}$  operators lead to observable single-quantum  $I_k$ -magnetization. Thus  $I_{kx}S_{\ell x}^2$  and  $I_{kx}S_{\ell y}^2$  both lead to  $(1/2, 1, 1/2)$  triplets. For  $S = 3/2$ , the product operators  $I_{kx}$ ,  $I_{kx}S_{\ell z}$ ,  $I_{kx}S_{\ell z}^2$  and  $I_{kx}S_{\ell z}^3$  represent quartets with amplitudes  $(1, 1, 1, 1)$ ,  $(-3/2, -1/2, 1/2, 3/2)$ ,  $(9/4, 1/4, 1/4, 9/4)$  and  $(-27/8, -1/8, 1/8, 27/8)$  respectively. In addition, the products  $I_{kx}S_{\ell x}^2$  and  $I_{kx}S_{\ell y}^2$  both lead to quartets with amplitudes  $(3/4, 7/4, 7/4, 3/4)$ .

## 11. SEMISELECTIVE AND SELECTIVE PULSES

*Semiselective* pulses with  $|2\pi J| < |\gamma B_1| < |\Delta\Omega|$ , i.e. pulses that affect all multiplet components of one given spin  $k$  uniformly, are simply represented by the operator  $\exp\{i\beta I_{kv}\}$  (i.e. by restricting the summation in eqn. (22) to a single spin). When applicable, the effect of the offset may be expressed in terms of tilted rf fields [eqns. (39)–(41)].

*Selective* pulses acting on individual multiplet lines, with  $|\gamma B_1| < |2\pi J| < |\Delta\Omega|$ , can be described by linear combinations of product operators. In a coupled two-spin system, one of the doublet components of spin  $k$  can be constructed by a linear combination of the operators  $I_{kx}$  and  $2I_{kx}I_{\ell z}$ , as may be appreciated by inspection of Fig. 4. Thus a selective pulse may be represented by the transformation

$$\sigma(t_+) = \exp\{-i\beta_{\frac{1}{2}}(I_{kx} \pm 2I_{kx}I_{\ell z})\}\sigma(t_-)\exp\{+i\beta_{\frac{1}{2}}(I_{kx} \pm 2I_{kx}I_{\ell z})\} \quad (99)$$

or in shorthand

$$\sigma(t_-) \xrightarrow{\beta_{\frac{1}{2}}(I_{kx} \pm 2I_{kx}I_{\ell z})} \sigma(t_+) \quad (100)$$

This transformation can be expanded as a sequence of rotations (see Section 6):

$$\sigma(t_-) \xrightarrow{-\frac{\pi}{2}I_{ky}} \xrightarrow{\frac{\beta}{2}I_{kz}} \xrightarrow{\pm\frac{\beta}{2}2I_{kz}I_{\ell z}} \xrightarrow{\frac{\pi}{2}I_{ky}} \sigma(t_+). \quad (101)$$

It follows that a selective pulse can be represented formally (or even generated experimentally) by a sequence of semiselective pulses in combination with a free precession period.<sup>(67)</sup> Equation (101) can be evaluated by the rules derived in Section 5.

Expressions analogous to eqns. (99)–(101) can easily be constructed for selective pulses in arbi-



trarily complex spin systems. In a three spin system ( $k, \ell, m$ ), the appropriate linear combinations of operators may be readily derived from the central part of Fig. 4. Thus a selective pulse affecting the  $k$ -spin transition corresponding to  $I_{\ell z} = I_{mz} = +1/2$  is described by the transformation

$$\sigma(t_-) \xrightarrow{\beta_4^1 [I_{kx} + 2I_{kx}I_{\ell z} + 2I_{kx}I_{mz} + 4I_{kx}I_{\ell z}I_{mz}]} \sigma(t_+). \quad (102)$$

When this expression is expanded in analogy to eqn. (101), the evolution under terms containing three operators must be computed, for example:

$$I_{kx} \xrightarrow{\beta_4^1 4I_{kz}I_{\ell z}I_{mz}} I_{kx} \cos(\beta/4) + 4I_{ky}I_{\ell z}I_{mz} \sin(\beta/4) \quad (103)$$

which represents a trivial extension of eqns. (17)–(20).

It is thus not necessary to take recourse to single transition operators although these provide an alternative approach to describe selective pulses.<sup>(4,7,48)</sup>

In the following sections, a number of selected examples will be discussed to illustrate the application of the operator formalism to different pulse experiments. Heteronuclear applications (INEPT and DEPT) have been treated elsewhere.<sup>(58)</sup>

## 12. TWO-DIMENSIONAL CORRELATION SPECTROSCOPY

Consider the basic two-dimensional (2D) correlation experiment shown in Fig. 10a, which has found widespread use for the identification of coupling partners in networks of coupled spins.<sup>(4,6,23,24)</sup> For a simple two-spin system, the density operator at various stages can be described as follows (the lower indices of  $\sigma_i$  refer to the points of time in Fig. 10):

$$\begin{aligned} \sigma_0 &= I_{kz} + I_{\ell z} \\ &\downarrow \frac{\pi}{2} (I_{kx} + I_{\ell x}) \\ \sigma_1 &= -I_{ky} - I_{\ell y} \end{aligned} \quad (104)$$

$$\begin{aligned} &\downarrow \Omega_k t_1 I_{kz} + \Omega_{\ell} t_1 I_{\ell z} + \pi J_{k\ell} t_1 2I_{kz}I_{\ell z} \\ \sigma_2 &= [-I_{ky} \cos \Omega_k t_1 + I_{kx} \sin \Omega_k t_1 \\ &\quad - I_{\ell y} \cos \Omega_{\ell} t_1 + I_{\ell x} \sin \Omega_{\ell} t_1] \cos \pi J_{k\ell} t_1 \\ &\quad + [2I_{kx}I_{\ell z} \cos \Omega_k t_1 + 2I_{ky}I_{\ell z} \sin \Omega_k t_1 \\ &\quad + 2I_{kz}I_{\ell x} \cos \Omega_{\ell} t_1 + 2I_{kz}I_{\ell y} \sin \Omega_{\ell} t_1] \sin \pi J_{k\ell} t_1 \end{aligned} \quad (105)$$

$$\begin{aligned} &\downarrow \frac{\pi}{2} (I_{kx} + I_{\ell x}) \\ \sigma_3^{\text{obs}} &= [I_{kx} \sin \Omega_k t_1 + I_{\ell x} \sin \Omega_{\ell} t_1] \cos \pi J_{k\ell} t_1 \\ &\quad - [2I_{ky}I_{\ell z} \sin \Omega_{\ell} t_1 + 2I_{kz}I_{\ell y} \sin \Omega_k t_1] \sin \pi J_{k\ell} t_1. \end{aligned} \quad (107)$$

In the last step only observable terms have been retained. The first term will continue to precess at  $\Omega_k \pm \pi J_{k\ell}$  in the detection period. Hence, after 2DFT, it will lead to a 2D multiplet pattern on the diagonal at  $\omega_1 = \omega_2 = \Omega_k$  with in-phase doublet structure (cosine-dependence on  $J_{k\ell}$ ) in both directions. Similarly, the second term leads to an in-phase diagonal multiplet at  $\omega_1 = \omega_2 = \Omega_{\ell}$ . The



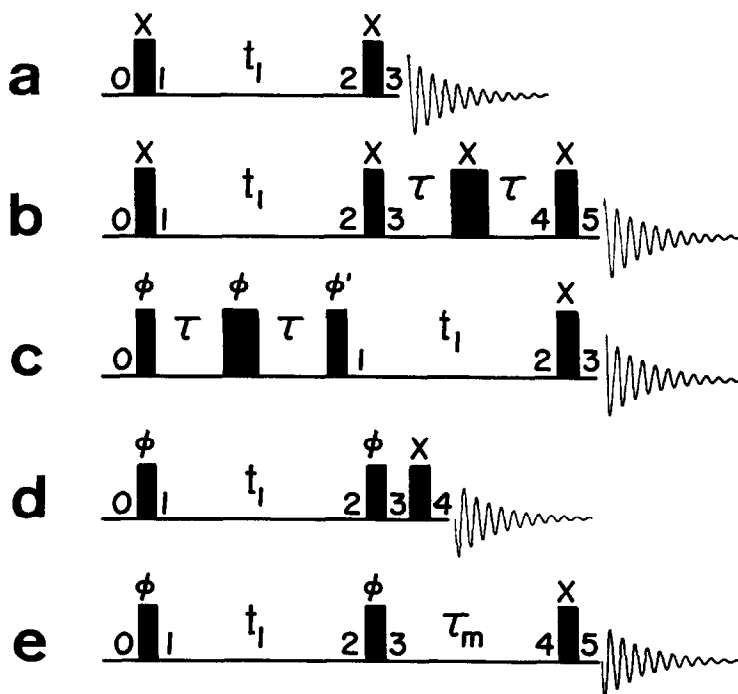


FIG. 10. Pulse sequences discussed in Sections 12–16. The pulse rotation angles ( $\pi/2$  or  $\pi$ ) are distinguished by the pulse widths, and the rf phases are indicated for the basic versions of the experiments. The numbers refer to the state of the system (density operator) as referred to in the text. (a) two-dimensional (2D) correlation spectroscopy, (b) 2D relayed magnetization transfer spectroscopy, (c) basic sequence for multiple quantum NMR, (d) 2D correlation spectroscopy with multiple quantum filter, and (e) 2D exchange spectroscopy. All sequences are shown for homonuclear applications but can be extended for heteronuclear cases.

third term, representing antiphase  $k$ -magnetization, will resume precession at  $\Omega_k \pm \pi J_{k\ell}$  in the detection period and therefore leads to a cross-peak multiplet at  $\omega_1 = \Omega_\ell$ ,  $\omega_2 = \Omega_k$  with antiphase doublet structure (sine-dependence on  $J_{k\ell}$ ) in both dimensions. The last term represents a cross-peak multiplet at  $\omega_1 = \Omega_k$  and  $\omega_2 = \Omega_\ell$ . Thus, eqn. (107) provides a concise and complete description of the basic 2D correlation experiment. The calculation can be simplified by treating the first two pulses and the  $t_1$  period as a composite rotation [see Section 6 and eqn. (55)]. Extensions to networks of coupled spins of arbitrary complexity are easily carried out.

### 13. RELAYED MAGNETIZATION TRANSFER

Recently, several experiments have been proposed which are based on relayed transfer of single quantum coherence between two nuclei  $k$  and  $m$  that are not coupled together but possess a common coupling partner  $\ell$ . Such experiments are used to assist in the identification of homonuclear coupling networks<sup>(33)</sup> and to identify neighbouring carbon-13 nuclei.<sup>(34–36)</sup>

One of the pulse sequences appropriate for homonuclear relayed transfer is shown in Fig. 10b, where  $\tau$  can be either a fixed or a variable interval. Consider a three-spin system ( $k, \ell, m$ ) with  $J_{km} = 0$ , where we shall focus attention on magnetization which starts precession at  $\Omega_k$  in  $t_1$  and ends up precessing at  $\Omega_m$  in  $t_2$ . After the second  $(\pi/2)_x$  pulse, the relevant terms are described by eqn. (107). Only the fourth term represents transverse antiphase  $\ell$  magnetization and can be subject to relayed



transfer from  $k$  to  $m$  via  $\ell$ :

$$\sigma_3^{(k \rightarrow \ell)} = -2I_{kz}I_{\ell y} \sin(\Omega_k t_1) \sin(\pi J_{k\ell} t_1). \quad (108)$$

In the subsequent  $2\tau$  interval in Fig. 10b, we need only consider the effect of scalar couplings, since chemical shifts are refocussed. To qualify for a transfer of coherence to the third  $m$  nucleus, the transverse  $\ell$ -magnetization in  $\sigma_3$  must evolve such as to be in-phase with respect to  $J_{k\ell}$  and antiphase with respect to  $J_{\ell m}$ . Only one term fulfills those conditions at the end of the  $2\tau$ -interval:

$$\sigma_4^{(k \rightarrow \ell)} = 2I_{\ell y}I_{mz} \sin(\Omega_k t_1) \sin(\pi J_{k\ell} t_1) \sin(\pi J_{k\ell} 2\tau) \sin(\pi J_{\ell m} 2\tau). \quad (109)$$

By the third pulse, this term is converted into transverse  $m$ -magnetization:

$$\sigma_5^{(k \rightarrow \ell \rightarrow m)} = -2I_{\ell z}I_{my} \sin(\Omega_k t_1) \sin(\pi J_{k\ell} t_1) \sin(\pi J_{k\ell} 2\tau) \sin(\pi J_{\ell m} 2\tau). \quad (110)$$

This term describes a cross-peak multiplet at  $\omega_1 = \Omega_k$  and  $\omega_2 = \Omega_m$  with antiphase doublet structure in both dimensions, and with an amplitude determined by the transfer function  $f(\tau)^{(k \rightarrow \ell \rightarrow m)} = \sin \pi J_{k\ell} 2\tau \sin \pi J_{\ell m} 2\tau$ . The presence of such a cross-peak in a 2D relayed spectrum provides conclusive evidence that the nuclei  $k$  and  $m$  belong to the same network of coupled spins.

#### 14. MULTIPLE QUANTUM SPECTROSCOPY

To illustrate the utility of operator techniques for the discussion of multiple quantum experiments, consider the pulse sequence shown in Fig. 10c, which has proven convenient for investigating homonuclear systems. To excite even-quantum coherences, the phases  $\varphi$  and  $\varphi'$  must be equal, whereas for odd-quantum experiments  $\varphi' = \varphi + \pi/2$ . For the suppression of undesired coherence  $p' \neq p$ ,  $\varphi$  is cycled through  $k(2\pi/2p)$  ( $k = 0, 1, \dots, (2p-1)$ ) while the signals are alternatively added and subtracted.<sup>(13)</sup> The effect of the excitation sandwich with a phase  $\varphi = \varphi'$  is described by eqn. (58). When applied to a system initially without coherence the complete experiment may be represented by the sequence

$$\sigma(0) \xrightarrow{\sum \pi J_{k\ell} 2\tau 2I_{ky}I_{\ell y}} \xrightarrow{\varphi \sum I_{kz}} \xrightarrow{\mathcal{H}t_1} \xrightarrow{\frac{\pi}{2} \sum I_{kx}} \xrightarrow{\mathcal{H}t_2} \sigma(t_1, t_2) \quad (111)$$

with the unperturbed Hamiltonian of eqn. (12).

At the beginning of the evolution period, assuming  $\varphi = 0$  (i.e. all excitation pulses along the x-axis) we obtain, according to eqn. (51), the following state for a two-spin system:

$$\sigma_1(\varphi = 0) = (I_{kz} + I_{\ell z}) \cos \pi J_{k\ell} 2\tau + (2I_{kx}I_{\ell y} + 2I_{ky}I_{\ell x}) \sin \pi J_{k\ell} 2\tau. \quad (112)$$

The second term represents pure double quantum coherence [eqn. (80)]. A phase shift  $\varphi = k(2\pi/4)$  [second term in the cascade of eqn. (111)] leaves the leading longitudinal terms of eqn. (112) invariant, while the double quantum coherence is invariant for  $k = 0$  and  $2$ , and reversed in sign for  $k = 1$  and  $3$  [eqn. (97)]. The evolution of the double quantum coherence, which is unaffected by the scalar coupling between the two nuclei, is described in analogy to eqn. (81):

$$\sigma_2 = [(2I_{kx}I_{\ell y} + 2I_{ky}I_{\ell x}) \cos(\Omega_k + \Omega_{\ell})t_1 - (2I_{kx}I_{\ell x} - 2I_{ky}I_{\ell y}) \sin(\Omega_k + \Omega_{\ell})t_1] \sin \pi J_{k\ell} 2\tau. \quad (113)$$

A mixing pulse with rotation angle  $\beta = \pi/2$  (see Fig. 10c) converts only the cosine-modulated term in eqn. (113) into observable magnetization:

$$\sigma_3^{\text{obs}} = (2I_{kx}I_{\ell z} + 2I_{kz}I_{\ell x}) \cos(\Omega_k + \Omega_{\ell})t_1 \sin \pi J_{k\ell} 2\tau. \quad (114)$$

The detected signals consist of antiphase multiplets at  $\omega_2 = \Omega_k$  and  $\Omega_{\ell}$ .

An observe pulse with flip angle  $\beta \neq \pi/2$  also converts part of the *sine*-modulated term in eqn. (113) into observable magnetization. This makes it possible to identify the sign of double quantum precession.<sup>(31)</sup> In extended coupling networks, however, this behaviour is restricted to situations where the multiple quantum coherence and the observable magnetization contain a common  $I_{kx}$  or  $I_{ky}$  operator.<sup>(62)</sup>



In linear three-spin systems ( $k, \ell, m$ ) with  $J_{km} = 0$ , the preparation sandwich may also produce terms of the form

$$\sigma_1 = -4I_{\ell z}I_{ky}I_{my} \sin 2\pi J_{k\ell}\tau \sin \pi J_{\ell m}2\tau. \quad (115)$$

This term consists of zero and double quantum coherence of spins  $k$  and  $m$  in antiphase with respect to the "central" spin  $\ell$ . This phenomenon can be used to prove that  $k$  and  $m$  belong to the same coupling network.<sup>(62)</sup> It is also possible to generate double quantum coherence involving two magnetically equivalent nuclei  $I_k$  and  $I_m$  via a coupling partner  $I_\ell$ , a phenomenon that can be used to identify the existence of magnetic equivalence in coupling networks. It is clear that antiphase magnetization terms such as in eqn. (115) can only become apparent in the spectrum when the couplings  $J_{ki}, J_{lm} \dots$  are resolved. This requirement is consistent with the coherence transfer selection rules discussed by Braunschweiler *et al.*<sup>(62)</sup>

## 15. MULTIPLE QUANTUM FILTERS

Recently, several experiments have been proposed which exploit coherence transfer via multiple quantum coherence to simplify single quantum spectra.<sup>(29,30,68)</sup> By way of example, consider the application of the product operator formalism to double quantum filters for simplifying 2D correlation spectra.<sup>(68)</sup> In the pulse sequence in Fig. 10d, the phase  $\varphi$  is cycled such as to retain only pure double quantum coherence between the second and third  $\pi/2$  pulses. The density operator of a two-spin system at the end of the evolution period has been given already in eqn. (106). After the second pulse (with the same rf phase  $\varphi = x$ ) we obtain:

$$\begin{aligned} \sigma_3 = & [-I_{kz} \cos \Omega_k t_1 + I_{kx} \sin \Omega_k t_1 - I_{\ell z} \cos \Omega_\ell t_1 + I_{\ell x} \sin \Omega_\ell t_1] \cos \pi J_{k\ell} t_1 \\ & - [2I_{kx}I_{\ell y} \cos \Omega_k t_1 + 2I_{ky}I_{\ell x} \cos \Omega_\ell t_1 + 2I_{kz}I_{\ell y} \sin \Omega_k t_1 \\ & + 2I_{ky}I_{\ell z} \sin \Omega_\ell t_1] \sin \pi J_{k\ell} t_1. \end{aligned} \quad (116)$$

Unlike eqn. (107), which describes only observable terms, this expression gives a complete description of the density operator, including longitudinal terms and two-spin coherence. The latter can be expressed as linear combinations of pure double and zero quantum coherences according to eqns. (80) and (83):

$$\begin{aligned} \sigma_3 = & [-I_{kz} \cos \Omega_k t_1 + I_{kx} \sin \Omega_k t_1 - I_{\ell z} \cos \Omega_\ell t_1 + I_{\ell x} \sin \Omega_\ell t_1] \cos \pi J_{k\ell} t_1 \\ & + \left\{ \frac{1}{2} [(2I_{kx}I_{\ell y} + 2I_{ky}I_{\ell x}) - (2I_{ky}I_{\ell x} - 2I_{kx}I_{\ell y})] \cos \Omega_k t_1 + \frac{1}{2} [(2I_{kx}I_{\ell y} \right. \\ & + 2I_{ky}I_{\ell x}) + (2I_{ky}I_{\ell x} - 2I_{kx}I_{\ell y})] \cos \Omega_\ell t_1 + 2I_{kz}I_{\ell y} \sin \Omega_k t_1 \\ & \left. + 2I_{ky}I_{\ell z} \sin \Omega_\ell t_1 \right\} \sin \pi J_{k\ell} t_1. \end{aligned} \quad (117)$$

In the course of the phase-cycle, all longitudinal, zero quantum and antiphase single quantum terms are cancelled, leaving a pure double quantum state:

$$\sigma_3^{2QT} = \left\{ \frac{1}{2} (2I_{kx}I_{\ell y} + 2I_{ky}I_{\ell x}) \cos \Omega_k t_1 + \frac{1}{2} (2I_{kx}I_{\ell y} + 2I_{ky}I_{\ell x}) \cos \Omega_\ell t_1 \right\} \sin \pi J_{k\ell} t_1. \quad (118)$$

The third pulse in Fig. 10d (with constant phase  $x$ ) generates single quantum magnetization:

$$\sigma_4^{\text{obs}} = \left\{ \frac{1}{2} (2I_{kx}I_{\ell z} + 2I_{kz}I_{\ell x}) \cos \Omega_k t_1 + \frac{1}{2} (2I_{kx}I_{\ell z} + 2I_{kz}I_{\ell x}) \cos \Omega_\ell t_1 \right\} \sin \pi J_{k\ell} t_1. \quad (119)$$

This expression may be compared with eqn. (107), which describes the observable part of a two-spin system at the beginning of the detection period in conventional 2D correlation spectroscopy. In contrast to eqn. (107), the operators giving rise to diagonal peaks [first and fourth terms in eqn. (119)] appear with antiphase doublet structure in both dimensions of the two-dimensional frequency domain. In spectra of large molecules such as biopolymers, where the linewidth may be comparable to the  $J$ -coupling, the diagonal signals will therefore be attenuated by partial cancellation of antiphase multiplets to the *same* extent as cross-peaks. In addition, diagonal signals stemming from singlets are removed, hence the dominant diagonal ridge of conventional correlation spectra is largely eliminated by the double quantum filter.



The second and third terms in eqn. (119) give rise to cross-peaks and hence carry information about coupling partners. These peaks appear with *half* the amplitude of those obtained in conventional correlation spectra.

## 16. ZERO-QUANTUM INTERFERENCE IN 2D EXCHANGE SPECTROSCOPY

Slow dynamic processes such as chemical exchange, transient Overhauser effects and spin-diffusion can be studied by two-dimensional exchange spectroscopy.<sup>(22)</sup> The appropriate pulse sequence, shown in Fig. 10e, is essentially the same as Fig. 10d, except for the extended mixing interval  $\tau_m$  and the phase cycle which selects the *longitudinal* polarization evolving in  $\tau_m$ , while coherences of order  $p = 1, 2, 3, \dots$  are suppressed.<sup>(69)</sup> Since zero-quantum coherence has the same response to rf phase-shifts as longitudinal polarization, it cannot be separated by phase-cycling.

Thus the relevant part of the density operator at the beginning of the mixing interval  $\tau_m$  comprises three terms of eqn. (117):

$$\sigma_3^{\text{longitudinal}+ZQT} = [-I_{kz} \cos \Omega_k t_1 - I_{\ell z} \cos \Omega_\ell t_1] \cos \pi J_{k\ell} t_1 \\ + (I_{ky} I_{\ell x} - I_{kx} I_{\ell y}) [\cos \Omega_\ell t_1 - \cos \Omega_k t_1] \sin \pi J_{k\ell} t_1. \quad (120)$$

The zero-quantum term evolves according to eqn. (84), while the longitudinal terms mix under the combined effects of exchange and relaxation. After the final pulse in Fig. 10e, the observable magnetization is:

$$\sigma_5^{\text{obs.}} = [I_{ky} a_{kk} \cos \Omega_k t_1 + I_{\ell y} a_{\ell\ell} \cos \Omega_\ell t_1 + I_{ky} a_{\ell k} \cos \Omega_\ell t_1 + I_{\ell y} a_{k\ell} \cos \Omega_k t_1] \cos \pi J_{k\ell} t_1 \\ + (I_{kz} I_{\ell x} - I_{kx} I_{\ell z}) \cos (\Omega_k - \Omega_\ell) \tau_m (\cos \Omega_\ell t_1 - \cos \Omega_k t_1) \sin \pi J_{k\ell} t_1 \quad (121)$$

for a symmetrical two-site exchange case, the mixing coefficients<sup>(38,69,70)</sup> are:

$$a_{kk} = a_{\ell\ell} = \frac{1}{2} \exp(-R_1 \tau_m) [1 + \exp(-2k \tau_m)] \quad (122)$$

$$a_{k\ell} = a_{\ell k} = +\frac{1}{2} \exp(-R_1 \tau_m) [1 - \exp(-2k \tau_m)] \quad (123)$$

with the spin-lattice relaxation rate  $R_1$  and the exchange rate  $k$ .

One immediately recognizes diagonal peaks proportional to  $a_{kk}$  and  $a_{\ell\ell}$ , exchange cross-peaks proportional to  $a_{\ell k}$  and  $a_{k\ell}$  (all of which are in-phase with respect to  $J_{k\ell}$ ), as well as antiphase diagonal- and cross-peaks that stem from zero-quantum coherence (so-called *J*-cross peaks in exchange spectra<sup>(69)</sup>).

A pulse with  $\beta \neq \pi/2$  at the end of the evolution period generates in addition terms of the type  $2I_{kz} I_{\ell z}$  (longitudinal two-spin order). The decay of such terms (dipolar relaxation in solids) may be monitored by an observation pulse with  $\beta \neq \pi/2$ . This leads to a 2D analogue of the Jeener-Broekaert experiment.<sup>(71)</sup>

## 17. SIGNAL INTENSITIES FOR NON-EQUILIBRIUM SYSTEMS

It is known that the signal intensities in pulse Fourier spectroscopy show surprising dependences on the pulse rotation angle when systems with non-equilibrium populations (non-equilibrium states of the first kind) are investigated.<sup>(5)</sup> Such states occur frequently in CIDNP and relaxation measurements. The rotation angle dependence of the signal intensities can be computed very easily with the product operator formalism.

Consider a weakly-coupled system of  $N$  spins  $\frac{1}{2}$  with non-equilibrium populations. The density matrix contains  $2^N$  diagonal elements, and may be expanded in the orthogonal set of  $2^N$  operators  $\{\mathbf{B}_s\}$  consisting of a unity operator  $\frac{1}{2}E$ ,  $N$  operators  $I_{kz}$ ,  $N-1$  operators  $2I_{kz} I_{\ell z} \dots$  and one  $N$ -spin operator. The coefficients of these operators can be readily expressed in terms of populations, for example in a two-spin system:

$$\sigma = \frac{1}{2} [(P_{\alpha\alpha} + P_{\alpha\beta} - P_{\beta\alpha} - P_{\beta\beta}) I_{1z} + (P_{\alpha\alpha} - P_{\alpha\beta} + P_{\beta\alpha} - P_{\beta\beta}) I_{2z} \\ + (P_{\alpha\alpha} - P_{\alpha\beta} - P_{\beta\alpha} + P_{\beta\beta}) 2I_{1z} I_{2z} + (P_{\alpha\alpha} + P_{\alpha\beta} + P_{\beta\alpha} + P_{\beta\beta}) \frac{1}{2} E]. \quad (124)$$



In a three-spin system, the coefficients are:

$$\begin{aligned}
 \sigma = \frac{1}{4} [ & (+P_{\alpha\alpha\alpha} + P_{\alpha\alpha\beta} + P_{\alpha\beta\alpha} - P_{\beta\alpha\alpha} + P_{\alpha\beta\beta} - P_{\beta\alpha\beta} - P_{\beta\beta\alpha} - P_{\beta\beta\beta})I_{1z} \\
 & + (+P_{\alpha\alpha\alpha} + P_{\alpha\alpha\beta} - P_{\alpha\beta\alpha} + P_{\beta\alpha\alpha} - P_{\alpha\beta\beta} + P_{\beta\alpha\beta} - P_{\beta\beta\alpha} - P_{\beta\beta\beta})I_{2z} \\
 & + (+P_{\alpha\alpha\alpha} - P_{\alpha\alpha\beta} + P_{\alpha\beta\alpha} + P_{\beta\alpha\alpha} - P_{\alpha\beta\beta} - P_{\beta\alpha\beta} + P_{\beta\beta\alpha} - P_{\beta\beta\beta})I_{3z} \\
 & + (+P_{\alpha\alpha\alpha} + P_{\alpha\alpha\beta} - P_{\alpha\beta\alpha} - P_{\beta\alpha\alpha} - P_{\alpha\beta\beta} - P_{\beta\alpha\beta} + P_{\beta\beta\alpha} + P_{\beta\beta\beta})2I_{1z}I_{2z} \\
 & + (+P_{\alpha\alpha\alpha} - P_{\alpha\alpha\beta} + P_{\alpha\beta\alpha} - P_{\beta\alpha\alpha} - P_{\alpha\beta\beta} + P_{\beta\alpha\beta} - P_{\beta\beta\alpha} + P_{\beta\beta\beta})2I_{1z}I_{3z} \\
 & + (+P_{\alpha\alpha\alpha} - P_{\alpha\alpha\beta} - P_{\alpha\beta\alpha} + P_{\beta\alpha\alpha} + P_{\alpha\beta\beta} - P_{\beta\alpha\beta} - P_{\beta\beta\alpha} + P_{\beta\beta\beta})2I_{2z}I_{3z} \\
 & + (+P_{\alpha\alpha\alpha} - P_{\alpha\alpha\beta} - P_{\alpha\beta\alpha} - P_{\beta\alpha\alpha} + P_{\alpha\beta\beta} + P_{\beta\alpha\beta} + P_{\beta\beta\alpha} - P_{\beta\beta\beta})4I_{1z}I_{2z}I_{3z} \\
 & + (+P_{\alpha\alpha\alpha} + P_{\alpha\alpha\beta} + P_{\alpha\beta\alpha} + P_{\beta\alpha\alpha} + P_{\alpha\beta\beta} + P_{\beta\alpha\beta} + P_{\beta\beta\alpha} + P_{\beta\beta\beta})\frac{1}{2}E].
 \end{aligned} \quad (125)$$

Each of the operators has a characteristic transformation behaviour under the action of an rf pulse with rotation angle  $\beta$ . In general, various orders of multiple quantum coherence are generated. In a single-pulse experiment, only product operators with a single transverse component need to be considered:

$$I_{kz} \xrightarrow{\beta \sum_k I_{ky}} I_{kx} \sin \beta \quad (126)$$

$$2I_{kz}I_{\ell z} \xrightarrow{\beta \sum_k I_{ky}} (2I_{kx}I_{\ell z} + 2I_{kz}I_{\ell x}) \sin \beta \cos \beta \quad (127)$$

$$4I_{kz}I_{\ell z}I_{mz} \xrightarrow{\beta \sum_k I_{ky}} (4I_{kx}I_{\ell z}I_{mz} + 4I_{kz}I_{\ell x}I_{mz} + 4I_{kz}I_{\ell z}I_{mx}) \sin \beta \cos^2 \beta. \quad (128)$$

Thus contributions from in-phase magnetization [eqn. (126)], which lead to multiplet lines of equal amplitude and sign, are proportional to  $\sin \beta$  and reach their maximum at  $\beta = \pi/2$ . However, antiphase multiplet magnetization, stemming from products of  $q$  operators, is proportional to  $\sin \beta \cos^{q-1} \beta$  and vanishes for  $\beta = \pi/2$  [eqns. (127), (128)]. For  $\beta = \pi/2$ , only in-phase magnetization survives and undistorted multiplets are obtained irrespective of the initial population state. On the other hand, if small rotation angles are used ( $\cos \beta \approx 1$ ), all product operators produce observable transverse magnetization. In this case the Fourier transform of the free induction signal is equivalent to the continuous-wave spectral response.<sup>(5)</sup>

## 18. CONCLUSIONS

The examples treated in the previous sections demonstrate the simplicity and usefulness of the product operator formalism discussed in this paper. For most practical situations, only a few rules, which have been summed up in Figs. 6–8, need to be retained. It is our experience that newcomers to the field of pulsed NMR, even with little understanding of quantum mechanics, very quickly get sufficiently familiar with this formalism to be able to analyse pulse experiments of arbitrary complexity. Many research workers have used operator approaches before; we have attempted here to present a treatment particularly appropriate for modern pulse experiments.

*Acknowledgements*—We are indebted to A. Wokaun and L. Braunschweiler for many stimulating discussions. O. W. Sørensen acknowledges support of the Danish Natural Science Research Council (J. Nr. 11–3294); M. H. Levitt acknowledges the Science and Engineering Research Council of Great Britain for a NATO Overseas Fellowship. We are grateful to Miss I. Müller for preparing many permutations of the manuscript. After submission of this work, we received manuscripts from F. J. M. van de Ven and C. W. Hilbers,<sup>(72)</sup> and from K. J. Packer and K. M. Wright,<sup>(73)</sup> who have both developed independently a similar operator formalism. We are grateful to these authors for making available their manuscripts prior to publication.



## REFERENCES

1. R. R. ERNST and W. A. ANDERSON, *Rev. Sci. Instrum.* **37**, 93 (1966).
2. H. Y. CARR and E. M. PURCELL, *Phys. Rev.* **94**, 630 (1954).
3. R. L. VOLD, J. S. WAUGH, M. P. KLEIN and D. E. PHELPS, *J. Chem. Phys.* **48**, 3831 (1968).
4. J. JEENER, Ampere Summer School, Basko Polje, Yugoslavia (1971).
5. S. SCHÄUBLIN, A. HÖHENER and R. R. ERNST, *J. Magn. Reson.* **13**, 196 (1974).
6. W. P. AUE, E. BARTHOLDI and R. R. ERNST, *J. Chem. Phys.* **64**, 2229 (1976).
7. W. P. AUE, J. KARHAN and R. R. ERNST, *J. Chem. Phys.* **64**, 4226 (1976).
8. G. BODENHAUSEN, R. FREEMAN, R. NIEDERMEYER and D. L. TURNER, *J. Magn. Reson.* **26**, 133 (1977).
9. G. BODENHAUSEN, R. FREEMAN and G. A. MORRIS, *J. Magn. Reson.* **23**, 171 (1976).
10. G. A. MORRIS and R. FREEMAN, *J. Magn. Reson.* **29**, 433 (1978).
11. H. HATANAKA, T. TERAOKA and T. HASHI, *J. Phys. Soc. Jpn.* **39**, 835 (1975).
12. S. VEGA and A. PINES, *J. Chem. Phys.* **66**, 5624 (1977).
13. A. WOKAUN and R. R. ERNST, *Chem. Phys. Lett.* **52**, 407 (1977).
14. A. A. MAUDSLEY and R. R. ERNST, *Chem. Phys. Lett.* **50**, 368 (1977).
15. A. A. MAUDSLEY, L. MÜLLER and R. R. ERNST, *J. Magn. Reson.* **28**, 463 (1977).
16. G. BODENHAUSEN and R. FREEMAN, *J. Magn. Reson.* **28**, 471 (1977).
17. G. A. MORRIS and R. FREEMAN, *J. Am. Chem. Soc.* **101**, 760 (1979).
18. G. A. MORRIS, *J. Am. Chem. Soc.* **102**, 428 (1980).
19. D. P. BURUM and R. R. ERNST, *J. Magn. Reson.* **39**, 163 (1980).
20. L. MÜLLER, *J. Am. Chem. Soc.* **101**, 4481 (1979).
21. G. BODENHAUSEN and D. J. RUBEN, *Chem. Phys. Lett.* **69**, 185 (1980).
22. J. JEENER, B. H. MEIER, P. BACHMANN and R. R. ERNST, *J. Chem. Phys.* **71**, 4546 (1979).
23. K. NAGAYAMA, ANIL KUMAR, K. WÜTHRICH and R. R. ERNST, *J. Magn. Reson.* **40**, 321 (1980).
24. A. BAX and R. FREEMAN, *J. Magn. Reson.* **44**, 542 (1981).
25. A. MINORETTI, W. P. AUE, M. REINHOLD and R. R. ERNST, *J. Magn. Reson.* **40**, 175 (1980).
26. G. BODENHAUSEN, R. L. VOLD and R. R. VOLD, *J. Magn. Reson.* **37**, 93 (1980).
27. M. H. LEVITT and R. FREEMAN, *J. Magn. Reson.* **33**, 473 (1979).
28. R. FREEMAN, S. P. KEMPSSELL and M. H. LEVITT, *J. Magn. Reson.* **38**, 453 (1980).
29. A. BAX, R. FREEMAN and S. P. KEMPSSELL, *J. Am. Chem. Soc.* **102**, 4849 (1980).
30. G. BODENHAUSEN and C. M. DOBSON, *J. Magn. Reson.* **44**, 212 (1981).
31. T. H. MARECI and R. FREEMAN, *J. Magn. Reson.* **48**, 158 (1982).
32. G. BODENHAUSEN, *Progr. Nucl. Magn. Reson. Spectrosc.* **14**, 137 (1981).
33. G. EICH, G. BODENHAUSEN and R. R. ERNST, *J. Am. Chem. Soc.* **104**, 3731 (1982).
34. P. H. BOLTON and G. BODENHAUSEN, *Chem. Phys. Lett.* **89**, 139 (1982).
35. P. H. BOLTON, *J. Magn. Reson.* **48**, 336 (1982).
36. H. KESSLER, M. BERND, H. KOGLER, J. ZARBOCK, O. W. SØRENSEN, G. BODENHAUSEN and R. R. ERNST, *J. Am. Chem. Soc.* in press.
37. G. L. HOATSON, K. J. PACKER and K. M. WRIGHT, *Mol. Phys.* **46**, 1311 (1982).
38. G. BODENHAUSEN and R. R. ERNST, *J. Am. Chem. Soc.* **104**, 1304 (1982).
39. P. MANSFIELD and P. G. MORRIS, *NMR Imaging in Biomedicine*, Academic Press, New York, 1982.
40. G. BODENHAUSEN and R. FREEMAN, *J. Magn. Reson.* **36**, 221 (1979).
41. U. FANO, *Rev. Mod. Phys.* **29**, 74 (1957).
42. C. P. SLICHTER, *Principles of Magnetic Resonance*, (2nd edition), Springer, Berlin, 1978.
43. K. BLUM, *Density Matrix Theory and Applications*, Plenum Press, New York, 1981.
44. A. MESSIAH, *Quantum Mechanics*, North-Holland, Amsterdam, 1961.
45. A. D. BAIN and S. BROWNSTEIN, *J. Magn. Reson.* **47**, 409 (1982).
46. B. C. SANCTUARY, *J. Chem. Phys.* **64**, 4352 (1976).
47. A. WOKAUN and R. R. ERNST, *J. Chem. Phys.* **67**, 1752 (1977).
48. S. VEGA, *J. Chem. Phys.* **68**, 5518 (1978).
49. G. L. HOATSON and K. J. PACKER, *Mol. Phys.* **40**, 1153 (1980).
50. G. BODENHAUSEN, R. FREEMAN, G. A. MORRIS and D. L. TURNER, *J. Magn. Reson.* **31**, 75 (1978).
51. A. ABRAGAM, *Principles of Nuclear Magnetism*, Oxford University Press, London, 1961.
52. A. ABRAGAM and M. GOLDMAN, *Nuclear Magnetism: Order and Disorder*, Oxford University Press, London, 1982.
53. U. HAEBERLEN, *High Resolution NMR in Solids, Selective Averaging*, Academic Press, New York, 1976.
54. R. FREEMAN, T. A. FRENKIEL and M. H. LEVITT, *J. Magn. Reson.* **44**, 409 (1981).
55. W. S. WARREN, D. P. WEITEKAMP and A. PINES, *J. Chem. Phys.* **73**, 2084 (1980).
56. W. K. RHIM, A. PINES and J. S. WAUGH, *Phys. Rev. B* **3**, 684 (1971).
57. D. M. DODDRELL, D. T. PEGG and M. R. BENDALL, *J. Magn. Reson.* **48**, 323 (1982).
58. O. W. SØRENSEN and R. R. ERNST, *J. Magn. Reson.* **51**, 477 (1983).
59. M. H. LEVITT, *J. Magn. Reson.* **48**, 234 (1982).
60. M. H. LEVITT, *J. Magn. Reson.* **50**, 95 (1982).
61. M. H. LEVITT and R. FREEMAN, *J. Magn. Reson.* **43**, 65 (1981).



62. L. BRAUNSCHWEILER, G. BODENHAUSEN and R. R. ERNST, *Mol. Phys.* **48**, 535 (1983).
63. L. MÜLLER and R. R. ERNST, *Mol. Phys.* **38**, 963 (1979).
64. M. H. LEVITT, G. BODENHAUSEN and R. R. ERNST, *J. Magn. Reson.* **53**, 443 (1983).
65. M. BLOOM, *Can. J. Phys.* **58**, 1510 (1980).
66. A. WOKAUN and R. R. ERNST, *Mol. Phys.* **36**, 317 (1978).
67. H. HATANAKA and C. S. YANNONI, *J. Magn. Reson.* **42**, 330 (1981).
68. U. PIANTINI, O. W. SØRENSEN and R. R. ERNST, *J. Am. Chem. Soc.* **104**, 6800 (1982).
69. S. MACURA, Y. HUANG, D. SUTER and R. R. ERNST, *J. Magn. Reson.* **43**, 259 (1981).
70. S. MACURA and R. R. ERNST, *Mol. Phys.* **41**, 95 (1980).
71. J. JEENER and P. BROEKAERT, *Phys. Rev.* **157**, 232 (1967).
72. F. J. M. VAN DE VEN and C. W. HILBERS, *J. Magn. Reson.* in press.
73. K. J. PACKER and K. M. WRIGHT, *Mol. Phys.* in press.